Scientific African 24 (2024) e02230

Contents lists available at ScienceDirect

Scientific African

journal homepage: www.elsevier.com/locate/sciaf

A fractional order Ebola transmission model for dogs and humans

Isaac K. Adu [a,*], Fredrick A. Wireko [c], Mojeeb Al-R. El-N. Osman [d], Joshua Kiddy K. Asamoah [b,c,*]

[a] Department of Mathematical Sciences, Kumasi Technical University, Kumasi, Ghana
[b] Department of Mathematics, Saveetha School of Engineering SIMATS, Chennai, India
[c] Department of Mathematics, Kwame Nkrumah University of Science and Technology, Kumasi, Ghana
[d] Department of Mathematics and Computer Science, International University of Africa, Sudan

ARTICLE INFO

Editor name: Ebenezer Bonyah

Keywords:
Caputo–Fabrizio derivative
Lagrange interpolation
Numerical simulation
Sumudu stability
Uganda Ebola data

ABSTRACT

Ebola is a serious disease that affects people; in many cases, it results in death. Ebola outbreaks have also occurred in communities where residents keep pets, particularly dogs. Due to a lack of food, the dogs must hunt for food. Dogs eat the internal organs of wildlife that the locals have killed and eaten, as well as small dead animals that are found within the communities which may contain the Ebola virus. This study introduces a mathematical model based on the Caputo–Fabrizio derivative to describe the Ebola transmission dynamics between dogs and humans. The model's existence and the uniqueness of its solution were investigated using fixed-point theory. Furthermore, through the Sumudu transform criterion, we established that the Caputo–Fabrizio Ebola model is Picard stable. Some qualitative analysis was also carried out to investigate the Ebola propagation trend in the dog-to-human model. The proposed model is fitted to the reported Ebola incidence in Uganda between October 15, 2022, and November 2, 2022. The Ebola reproduction number obtained using the cumulative data was 2.65. It is noticed that as the fractional order reduces, the Ebola reproduction number also reduces. We derived a numerical scheme for our model using the two-step Lagrange interpolation. It has been discovered that the fractional orders significantly influence the model, indicating that natural occurrences could affect the dynamics of Ebola. It is observed that when the recovery rate is enhanced, such as through the hospitalisation of Ebola-infected individuals, the disease will reduce. Finally, as we ensure a reduction in the contact rate among the dog's compartments, the disease does not spread adiabatically. Therefore, we urge that quarantine measures be put in place to control interactions among the dogs during the outbreak.

Introduction

Ebola is a severe and lethal infection that affects people. People contract Ebola by coming into contact with infected animals and objects like garments or sheets that have been exposed to an infected person's bodily fluids. Studies have shown that non-human primates and domestic dogs can contract Ebola. Many dogs licked the vomit of Ebola-infected patients, while others consumed the corpses of dead Ebola-infected animals [1–3]. Furthermore, these animals may also contract the Ebola virus by eating contaminated fruits partially eaten by Ebola-infected bats [3,4]. Ebola outbreaks have also occurred in communities where residents keep pets, particularly dogs. Due to a lack of food, the dogs must hunt for food. Dogs eat the internal organs of wildlife that the locals have killed and eaten, as well as small dead animals that are found within the communities. In the vast forest area, certain dogs are also

* Corresponding authors.
E-mail addresses: isaac.kadu@kstu.edu.gh (I.K. Adu), jkkasamoah@knust.edu.gh (J.K.K. Asamoah).

https://doi.org/10.1016/j.sciaf.2024.e02230
Received 13 October 2023; Received in revised form 27 March 2024; Accepted 2 May 2024
Available online 7 May 2024

used for hunting [1]. Dogs can be infected with Ebola; however, based on 2005 research conducted in Gabon during the epidemic, infected dogs are asymptomatic, meaning dogs can harbour the virus but are not infected by it [3,5]. In the early stages of their infection, dogs can spread Ebola to people and other animals by biting, licking, and other means. Ebola may potentially spread when people are exposed to the urine or faeces of sick pets. However, the dog is no longer contagious after its immune system eliminates it. Dogs do not die from the Ebola virus infection [3,5]. Several epidemiological studies have been undertaken to examine the spread of Ebola using a deterministic approach [6–12]. In contemporary biology, a significant proportion of biological systems have the capacity for memory or the manifestation of aftereffects. Hence, using fractional-order derivatives in the mathematical modelling of biological systems offers several notable benefits. Empirical evidence has demonstrated that the cell membranes of numerous biological species exhibit electrical conductivity characterised by fractional-order behaviour, manifesting as a collection of non-integer models. Fractional derivatives are employed to analyse the behaviour of these physical models efficiently.

Among the few researchers who have researched on Ebola with fractional order derivatives are Farman et al. [13], who developed a nonlinear time-fractional mathematical model of the Ebola epidemic to comprehend the spread of the disease. The work in [13] employed Caputo and Atangana–Baleanu fractional derivative operators, the fixed-point theorem, iterative schemes, the Laplace Adomian Decomposition technique, and numerical solutions. The author in [13] posited that the analysis presented in their work can help control or reduce Ebola in communities. Another model that is of great importance to this model is the model proposed by [14]. The researchers employed the Atangana–Baleanu derivative operator to expand the fractional order model of the Ebola virus among the bat population. A comprehensive rationale is provided for resolving the challenges posed by the fractional mathematical model, encompassing its existence and the uniqueness and stability of the proposed model. The stated model's solution is discovered numerically, and the outcomes are graphically displayed. Almugrin et al. [14] concluded that fractional derivatives can be used to understand the mathematical model. In 2021, Pan et al. [15], used a fractional order to study Ebola disease. They also studied positivity, the threshold quantity, and equilibrium points. The modified grid approximation method (MGAM) and the Gorenflo–Mainardi–Moretti–Paradisi scheme (GMMP) are used to find the numerical answer to the SEIR fractional order Ebola model. They concluded that their current fractional orders, parameters, and root-mean-square relative error $g(U) = 0.4146$ are more accurate representations of the actual data than the models presented in the related works. A fourth model related to the current study is [16]. They proposed an efficient computer method to numerically solve the fractional Ebola model, demonstrating its effectiveness across various time domains. Others are [13,17–21]. Fractional models utilise distinct mathematical tools and methodologies for solving equations and examining systems, which diverge from conventional calculus. Fractional calculus provides a more thorough comprehension of phenomena that display non-local and memory-dependent behaviour. In light of these, many researchers have proposed fractional models to study the dynamics of many infectious diseases; see, for example, [22–28]. Though the related works reviewed present interesting results about Ebola and its control, the dynamics of how Ebola spreads among domestic dogs and other non-human primates, on the other hand, and how Ebola is transmitted from domestic dogs to humans and vice versa have received no attention. In the current study, we considered dog-human Ebola transmission using Caputo Fabrizio derivatives. The Caputo–Fabrizio fractional derivative is a mathematical technique employed to characterise non-local and memory-dependent phenomena in diverse systems. In contrast to classical derivatives, fractional derivatives represent events characterised by intricate dynamics, memory effects, and non-local behaviours. The Caputo and Fabrizio fractional derivative, a specific derivative, has garnered interest due to its ability to maintain physical consistency and causality while modelling real-world systems. It is precious for explaining viscoelastic materials, fractional-order control systems, anomalous diffusion, and numerous biological systems in which memory effects are essential. The Caputo–Fabrizio fractional derivative is very useful because it can deal with initial conditions in a good way, which means that the physical meaning of the derivative is kept in real-world situations. It offers a mathematical framework for describing intricate behaviours in which the memory of former states influences the current dynamics of a system [29,30]. In addition, we incorporate a saturated incidence rate in the model since its use is believed to be more logical than bilinear incidence. Moreover, it includes the crowding effect and behavioural modifications and prohibits the selection of the appropriate parameters because the transmission rate is not bounded [31].

The subsequent components of the research are classified into the following categories: Section "Some Fundamental Notions" comprises the foundational components of the model. In Section "The classical integer order model" of this paper, we present the Ebola integer model. Describing the model as a whole, listing its presumptions, and giving the equations that make up the model serve as its outline. In Section "Model in fractional operator", the Ebola fractional model was presented, and its properties of positivity and boundedness were examined. Once again, in Section "Qualitative studies of the Ebola model", we comprehensively examine the model through qualitative analysis. The application of the Sumudu stability criterion was subsequently employed to analyse the model discussed in Section "Sumudu Transform Stability Criterion". In Section "Parameter estimation and numerical simulations", we presented the parameter estimation and numerical simulations. The research was completed in its entirety in Section "Conclusion".

Some fundamental notions

Definition 1 (*[32]*). Given that $M \in \mathcal{X}^1(\mho_1, \mho_2)$ where $\mho_2 > \mho_1$ and the fractional order is defined in the domain $\wp \in (0, 1)$. Then, the Caputo–Fabrizio derivative of order $\wp$ for the operator M is given by

$$^{CF}D_0^{\wp}D(t) = \frac{\mathcal{G}(\wp)}{(1-\wp)}\int_{\mho_2}^{t} exp\left(\frac{-\wp}{1-\wp}(t-\tau)\right)M'(\tau)d\tau,$$

where $t \geq 0$ and with the normalisation function $\mathcal{G}(\wp)$ that comes from $\wp$ and $\mathcal{G}(0) = \mathcal{G}(1) = 1$.

Definition 2 ([33]). From the definition above, if we define $M \in \mathcal{X}^1(\mho_1, \mho_2)$ and $\wp \in (0,1)$. Then the Caputo–Fabrizio derivative of order $\wp$ is redefined for $M \in L^1(-\infty, \mho_2)$ in the form;

$$^{CF}D_0^{\wp}M(t) = \frac{\wp\mathcal{G}(\wp)}{(1-\wp)}\int_{-\infty}^{\mho}[M(t)-M(\tau)]exp\left(\frac{-\wp}{1-\wp}(t-\tau)\right)d\tau.$$

Definition 3 ([33]). We then define the Caputo–Fabrizio integral operator by

$$^{CF}I^{\wp}M(t) = \frac{2(1-\wp)}{(2-\wp)(\mathcal{G}(n))}M(t) + \frac{2\wp}{(2-\wp)(\mathcal{G}(n))}\int_0^t M(\tau)d\tau, \quad 0 < \wp < 1. \tag{1}$$

Definition 4 ([34–36]). From the classical Fourier integral, the Sumudu transform is formulated. Let us consider the set

$$\mathcal{B} = \left\{\mathcal{M} : \exists \mu, \alpha_1, \alpha_2 \geq 0, |M(t)| < \mu\, exp\left(\frac{t}{\alpha_j}\right), t \in [-1]^n \times [0,\infty)\right\}.$$

The Sumudu transform is then defined as the transformation of the operator $M \in \mathcal{B}$,

$$M(x) = \mathcal{ST}[M(t);x] = \frac{1}{x}\int_0^{\infty} exp\left(\frac{-t}{x}\right)M(t)dt, \quad [x \in (-\alpha_1, \alpha_2)].$$

For all values of t greater than or equal to zero, the inverse Sumudu transform of the function $M(x)$ may be expressed as $M(t) = \mathcal{ST}^{-1}[M(x)]$.

Definition 5 ([34]). We define the Sumudu transform in the Caputo sense by

$$\mathcal{ST}[^C D^{\wp}M(t);x] = x^{-\wp}\left(M(x) - \sum_{i=0}^{n} x^{\wp-i}[^C D^{\wp-i}M(t)]_{t=0}\right),$$

for the fractional value as an element $\wp$ of $[n-1, n]$.

Definition 6 ([37]). Let us consider the hypothetical existence of the derivative of Caputo–Fabrizio with a given operator denoted as M. The Sumudu transform of the operator, M, is subsequently defined using the Caputo–Fabrizio fractional derivative.

$$\mathcal{ST}[^C D_{0,t}^{\wp}M[t];x] = \frac{\mathcal{G}(\wp)}{1-\wp+\wp x}[\mathcal{ST}(M[t]) - M(0)].$$

The classical integer order model

We formulate the deterministic Ebola transmission model in this section. The model comprises two types of populations: humans and dogs. The entire human populace is given by $N_H(t)$, which is further grouped into four sub-classes: susceptible $S_H(t)$, exposed $E_H(t)$, symptomatic $I_H(t)$, and recovered $R_H(t)$ at time t. The entire dog populace is given by $N_D(t)$, which is also grouped into four sub-classes: susceptible $S_D(t)$, exposed $E_D(t)$, symptomatic $I_D(t)$, and recovered $R_D(t)$ at time t. m_1 represents the recruitment rate of humans, and that of dogs is denoted as m_2. β_H is the transmission rate of humans, and that of dogs is denoted by β_D. The proportion of antibodies humans generate in reaction to the occurrence of infection caused by dogs is represented by α_1. The proportion of antibodies dogs generate in reaction to the occurrence of infection caused by humans is denoted as α_2. The natural mortality in humans is represented by μ_H, μ_D is the natural mortality rate of dogs, δ_H represents the Ebola-induced death rate in humans, γ_H is the recovery rate of humans and γ_D is the recovered rate of dogs. The transfer rate of recovered humans to the susceptible human class is denoted by η_H; η_D represents the transfer rate of recovered dogs to the susceptible dog class, σ_H is the transfer rate of Ebola exposed humans to infectious class, σ_D is the transfer rate of Ebola-exposed dogs to the symptomatic dog class. The following assumptions support the developed dog-to-human Ebola model:

i. Susceptible dogs can become infected with Ebola through any of the following means: licking the vomit and bodies of Ebola-infected patients, consuming the fresh remains of dead Ebola-infected animals brought back to the villages, and or eating contaminated fruits that Ebola-infected bats have partially eaten.
ii. Susceptible humans can become infected with Ebola through one of the following means: being licked by an Ebola-infected dog, close contact with infected animals, or infected persons' clothes and bodily fluids.
iii. Ebola is spread to susceptible dogs from infected humans, and vice versa.
iv. Dogs do not suffer from Ebola-related deaths.

Table 1
Model parameters descriptions.

Parameters	Description
m_1	Recruitment rate of humans
m_2	Recruitment rate of dogs
β_H	Transmission rate from dogs to humans
β_D	Transmission rate from humans to dogs
α_1	Percentage of antibodies produced by humans in reaction to infection generated by dogs
α_2	Percentage of antibodies produced by dogs in reaction to infection generated by humans
μ_H	Natural mortality rate of humans
μ_D	Natural mortality rate of dogs
δ_H	Ebola-related death rate in humans
γ_H	Recovered rate of humans
γ_D	Recovered rate of dogs
η_H	Transfer rate of recovered humans to susceptible human class
η_D	Transfer rate of recovered dogs to susceptible dog class
σ_H	Transfer rate of Ebola exposed humans to symptomatic human class
σ_D	Transfer rate of Ebola exposed dogs to symptomatic dog class

These assumptions above are supported by [1–4,38]. The following eight (8) integer-order differential equations were generated based on the model descriptions and assumptions.

$$\begin{aligned}
\frac{dS_H}{dt} &= m_1 - \frac{\beta_H S_H I_D}{1+\alpha_1 I_D} - \mu_H S_H + \eta_H R_H,\\
\frac{dE_H}{dt} &= \frac{\beta_H S_H I_D}{1+\alpha_1 I_D} - (\mu_H + \sigma_H)E_H,\\
\frac{dI_H}{dt} &= \sigma_H E_H - (\gamma_H + \delta_H + \mu_H)I_H,\\
\frac{dR_H}{dt} &= \gamma_H I_H - (\eta_H + \mu_H)R_H,\\
\frac{dS_D}{dt} &= m_2 - \frac{\beta_D S_D I_H}{1+\alpha_2 I_H} - \mu_D S_D + \eta_D R_D,\\
\frac{dE_D}{dt} &= \frac{\beta_D S_D I_H}{1+\alpha_2 I_H} - (\sigma_D + \mu_D)E_D,\\
\frac{dI_D}{dt} &= \sigma_D E_D - (\gamma_D + \mu_D)I_D,\\
\frac{dR_D}{dt} &= \gamma_D I_D - (\eta_D + \mu_D)R_D,
\end{aligned} \tag{2}$$

where Eq. (2) is subjected to the following non-negative state variables:

$$S_H(0) = S_H^0, E_H(0) = E_H^0, I_H(0) = I_H^0, R_H(0) = R_H^0, S_D(0) = S_D^0, E_D(0) = E_D^0, I_D(0) = I_D^0, R_D(0) = R_D^0,$$

that is,

$$\inf(S_H(0), E_H(0), I_H(0), I_{S0}, R_H(0), R_0, S_D(0), E_D(0), I_D(0), R_D(0)) \geq 0.$$

This model employs a saturated incidence rate, as in the case of [39–41]. In the model, $\frac{\beta_H S_H I_D}{1+\alpha_1 I_D}$ and $\frac{\beta_D S_D I_H}{1+\alpha_2 I_H}$ are introduced as the saturated incidence rate to measure the saturation effect when I_D and I_H increase without bound. Here, $\beta_H I_D$ measures the force of infection in the case when the Ebola is introduced into the susceptible human population, whereas $\beta_D I_H$ measures the force of infection when the Ebola enters into the susceptible dog population. Moreover, $\frac{1}{1+\alpha_1 I_D}$ and $\frac{1}{1+\alpha_2 I_H}$ measure the inhibition effect of the behavioural changes in the susceptible human and dog populations that may occur as a result of the crowding effect of the infectious humans and dogs. Table 1 fully describes the model's parameters.

Model in fractional operator

This section introduces the fractional order model. A fractional order model is necessary because non-integer models can capture history, nonlocal effects and memory effects, which is key in biological systems [42]. Hence, the integer order Ebola model (2) is

reformulated as a fractional order system in Caputo–Fabrizio (CF) operator as follows;

$$\begin{aligned}
{}^{CF}D_0^{\wp} S_H(t) &= m_1^{\wp} - \frac{\beta_H^{\wp} S_H I_D}{1+\alpha_1 I_D} - \mu_H^{\wp} S_H + \eta_H^{\wp} R_H,\\
{}^{CF}D_0^{\wp} E_H(t) &= \frac{\beta_H^{\wp} S_H I_D}{1+\alpha_1 I_D} - (\mu_H^{\wp} + \sigma_H^{\wp}) E_H,\\
{}^{CF}D_0^{\wp} I_H(t) &= \sigma_H^{\wp} E_H - (\gamma_H^{\wp} + \delta_H^{\wp} + \mu_H^{\wp}) I_H,\\
{}^{CF}D_0^{\wp} R_H(t) &= \gamma_H^{\wp} I_H - (\eta_H^{\wp} + \mu_H^{\wp}) R_H,\\
{}^{CF}D_0^{\wp} S_D(t) &= m_2^{\wp} - \frac{\beta_D^{\wp} S_D I_H}{1+\alpha_2 I_H} - \mu_D^{\wp} S_D + \eta_D^{\wp} R_D,\\
{}^{CF}D_0^{\wp} E_D(t) &= \frac{\beta_D^{\wp} S_D I_H}{1+\alpha_2 I_H} - (\sigma_D^{\wp} + \mu_D^{\wp}) E_D,\\
{}^{CF}D_0^{\wp} I_D(t) &= \sigma_D^{\wp} E_D - (\gamma_D^{\wp} + \mu_D^{\wp}) I_D,\\
{}^{CF}D_0^{\wp} R_D(t) &= \gamma_D^{\wp} I_D - (\eta_D^{\wp} + \mu_D^{\wp}) R_D,
\end{aligned} \tag{3}$$

with the starting point values of the state variables; $S_H(0) = S_H^0, E_H(0) = E_H^0, I_H(0) = I_H^0, R_H(0) = R_H^0, S_D(0) = S_D^0, E_D(0) = E_D^0, I_D(0) = I_D^0$ and $R_D(0) = R_D^0$, and $0 < \wp < 1$ indicates the non-integer or fractional order of the Caputo–Fabrizio fractional derivative, ${}_0^{CF}D_t^{\wp}$. This operator is well known in studying biological systems that exhibit exponential lag or are very efficient in studying systems with lag time [42].

Qualitative studies of the Ebola model

A collection of qualitative studies about the Ebola model is presented in the current section.

Positivity and boundedness of the Ebola model

This part pertains to the comprehensive analysis that verifies the positivity and boundedness of the Ebola model.

Theorem 1. *Considering the initial values of the state variables* $\{S_H(0), E_H(0), I_H(0), R_H(0), S_D(0), E_D(0), I_D(0), R_D(0)\}$ *belonging to the set* $\mathcal{G}$*, and assuming the existence of the solutions* $\{S_H, E_H, I_H, R_H, S_D, E_D, I_D, R_D\}$*, it can be inferred in a manner that every solution is positive for all* t *equal to zero or more.*

Proof. Following the approach used in [43–46], we highlight some important properties that will help us prove the positivity of the Ebola model. By considering the norm,

$$\|\Psi\|_{\infty} = \sup_{t\in D_{\Psi}} |\Psi(t)|. \tag{4}$$

Where D_{Ψ} denotes the region of Φ.

Let us commence the proof with the susceptible human compartment, $S_H(t)$ for every $t \geq 0$, this leads to;

$$\begin{aligned}
{}^{FFP}D_{0,t}^{\wp} S_u(t) &\geq m_1^{\wp} - \frac{\beta_H^{\wp} S_H I_D}{1+\alpha_1 I_D} - \mu_H^{\wp} S_H + \eta_H^{\wp} R_H,\\
&\geq m_1^{\wp} - \beta_H^{\wp} S_H I_D - \mu_H^{\wp} S_H + \eta_H^{\wp} R_H,\\
&\geq -(\mu_H^{\wp} + \beta_H^{\wp} |\mathcal{Y}|) S_H,\\
&\geq -(\mu_H^{\wp} + \beta_H^{\wp} \sup_{t\in D_{\lambda}} |\mathcal{Y}|) S_H,\\
&\geq -(\mu_H^{\wp} + \beta_H^{\wp} \parallel \mathcal{Y} \parallel_{\infty}) S_H,
\end{aligned} \tag{5}$$

this, therefore, yields:

$$S_H(t) \geq S_H(0) \mathcal{Q}_{\wp} \left[-\frac{\xi^{1-\wp} \wp (\sigma_u^{\wp} + (\mu_H^{\wp} + \beta_H^{\wp}) \parallel \mathcal{G} \parallel_{\infty}) t^{\wp}}{M(\wp) - (1-\wp)(\mu_H^{\wp} + \beta_H^{\wp}) \parallel \mathcal{G} \parallel_{\infty}} \right]. \tag{6}$$

In the given context, the symbol ξ indicates the component of time. Hence, it can be observed that the susceptible human compartment, denoted as $S_H(t)$ in the Ebola model, maintains a positive value for all time instances $t \geq 0$. Furthermore, we take into account the exposed human compartment, denoted as $E_H(t)$, in our analysis:

$$\begin{aligned}
{}^{FFP}D_{0,t}^{\wp} E_u(t) &= \frac{\beta_H^{\wp} S_H I_D}{1+\alpha_1 I_D} - (\mu_H^{\wp} + \sigma_H^{\wp}) E_H,\\
&\geq -(\mu_H^{\wp} + \sigma_H^{\wp}) E_H,\\
E_H(t) &\geq E_H(0) \mathcal{Q}_{\wp} \left[-\frac{\xi^{1-\wp} \wp (\sigma_u + (\mu_H^{\wp} + \sigma_H^{\wp})) t^{\wp}}{M(\wp) - (1-\wp)(\mu_H^{\wp} + \sigma_H^{\wp})} \right].
\end{aligned} \tag{7}$$

Hence, it can be unequivocally said that the exposed human compartment, denoted as $E_u(t)$, exhibits positive values for all time instances t greater than or equal to zero. The positivity of the other state variables has been similarly demonstrated and is presented below.

$$\begin{aligned}
I_H(t) &\geq I_H(0)\mathcal{Q}_{\wp}\left[-\frac{\xi^{1-\wp}\wp(\gamma_H^{\wp}+\delta_H^{\wp}+\mu_H^{\wp})t^{\wp}}{M(\wp)-(1-\wp)(\gamma_H^{\wp}+\delta_H^{\wp}+\mu_H^{\wp})}\right],\\
R_H(t) &\geq J_u(0)\mathcal{Q}_{\wp}\left[-\frac{\xi^{1-\wp}\wp(\eta_H^{\wp}+\mu_H^{\wp})t^{\wp}}{M(\wp)-(1-\wp)(\eta_H^{\wp}+\mu_H^{\wp})}\right],\\
S_D(t) &\geq S_D(0)\mathcal{Q}_{\wp}\left[-\frac{\xi^{1-\wp}\wp(\sigma_u+(\mu_D^{\wp}+\beta_D^{\wp})||\mathcal{G}\,||_{\infty})t^{\wp}}{M(\wp)-(1-\wp)(\mu_D^{\wp}+\beta_D^{\wp})||\mathcal{G}\,||_{\infty}}\right],\\
E_D(t) &\geq E_D(0)\mathcal{Q}_{\wp}\left[-\frac{\xi^{1-\wp}\wp(\sigma_D^{\wp}+\mu_D^{\wp})t^{\varphi}}{M(\wp)-(1-\wp)(\sigma_D^{\wp}+\mu_D^{\wp})}\right],\\
I_D(t) &\geq I_D(0)\mathcal{Q}_{\varphi}\left[-\frac{\xi^{1-\wp}\upsilon(\gamma_D^{\wp}+\mu_D^{\wp})t^{\wp}}{M(\wp)-(1-\wp)(\gamma_D^{\wp}+\mu_D^{\wp})}\right],\\
R_D(t) &\geq R_D(0)\mathcal{Q}_{\varphi}\left[-\frac{\xi^{1-\wp}\wp(\eta_D^{\wp}+\mu_D^{\wp})t^{\wp}}{M(\wp)-(1-\wp)(\eta_D^{\wp}+\mu_D^{\wp})}\right].
\end{aligned} \tag{8}$$

The statement holds for all values of time greater than or equal to zero, thereby satisfying the positivity requirement of the Ebola model.

Theorem 2. *The solutions of the Ebola model, as represented by Eq. (1), the variables* $(S_H^{***}, E_H^{***}, I_H^{***}, R_H^{***}, S_D^{***}, E_D^{***}, I_D^{***}, R_D^{***})$ *represent the susceptible, the exposed, the infected, and the recovered individuals in the humans and dogs populations with given a set of positive initial conditions. Hence, it can be asserted that all solutions of the Ebola model exhibit bounded behaviour.*

Proof. It has been previously demonstrated that the solutions to the Ebola model exhibit positivity for all $t \geq 0$. By employing the methodology outlined in [47], we establish the boundedness of the Ebola model. The equation representing the human population is given by $\mathcal{F} = S_H + E_H + I_H + R_H$ leads to:

$${}^{FFP}\mathcal{D}_{0,t}^{\wp}\mathcal{F}(t) = m_1^{\wp} - \mu_H^{\wp}N_H + \delta_H^{\wp}I_H.$$

This suggests that

$${}^{FFP}\mathcal{D}_{0,t}^{\wp}\mathcal{F}(t) \leq m_1^{\wp} - \mu_H^{\wp}N_H,$$

thus, we have

$$\Psi_H^{\wp} = \{S_H, E_H, I_H, R_H \in \mathbb{R}_+^4 | \mathcal{F} \leq \frac{m_1^{\wp}}{\mu_H^{\wp}}\}.$$

Also for the dog population, we have $\mathcal{K} = S_D + E_D + I_D + R_D$, consequently, this leads to:

$${}^{FFP}\mathcal{D}_{0,t}^{\wp}\mathcal{K}(t) \leq m_2^{\wp} - \mu_D^{\wp}N_D,$$

and we have

$$\Psi_D^{\wp} = \left\{S_D, E_D, I_D, R_D \in \mathbb{R}_+^4 | \mathcal{K} \leq \frac{m_2^{\wp}}{\mu_D^{\wp}}\right\}.$$

Hence, it may be concluded that all solutions of the model exhibit positive invariance, given the initial values of the state variables within the domain $\Psi^{\wp}$ for any $t \geq 0$.

Ebola-free equilibrium and reproduction number

Ebola-free equilibrium

System (3) has an Ebola-free equilibrium and is denoted by

$$E_0 = \left(\frac{m_1^{\wp}}{\mu_H^{\wp}}, 0, 0, 0, \frac{m_2^{\wp}}{\mu_D^{\wp}}, 0, 0, 0\right).$$

We follow this by computing the basic reproduction number following the approach in [48].

The Ebola reproduction number ($\mathcal{R}_0$)

In the present section, we concentrate on the epidemiological threshold computation of the Ebola model using the next generation matrix technique as indicated by [49,50], and used by authors such as [51,52]. We define $\mathcal{R}_0$ as the absolute supremum of its eigenvalues denoted by $\mathcal{F}\mathcal{V}^{-1}$. Therefore, we define the threshold quantity by

$$\mathcal{R}_0 = \rho(\mathcal{F}\mathcal{V}^{-1}). \tag{9}$$

Now, from Eq. (9), we have

$$\mathcal{F} = \begin{pmatrix} \frac{\beta_H^{\wp} S_H I_D}{1+\alpha_1 I_D} \\ 0 \\ \frac{\beta_D^{\wp} S_D I_H^{\wp}}{1+\alpha_2 I_H} \\ 0 \end{pmatrix} \quad \text{and} \quad \mathcal{V} = \begin{pmatrix} (\mu_H^{\wp} + \sigma_H^{\wp}) E_H \\ -\sigma_H^{\wp} E_H + (\gamma_H^{\wp} + \delta_H^{\wp} + \mu_H^{\wp}) I_H \\ (\sigma_D^{\wp} + \mu_D^{\wp}) E_D \\ -\sigma_D^{\wp} E_D + (\gamma_D^{\wp} + \mu_D^{\wp}) I_D \end{pmatrix}. \tag{10}$$

Solving the above using the steps given in [49,50], the Ebola reproduction number is given as:

$$\mathcal{R}_0 = \sqrt{\frac{\beta_D^{\wp}\beta_H^{\wp} m_1^{\wp} m_2^{\wp} \sigma_D^{\wp} \sigma_H^{\wp}}{\mu_D^{\wp}\mu_H^{\wp}\left(\gamma_D^{\wp}+\mu_D^{\wp}\right)\left(\sigma_D^{\wp}+\mu_D^{\wp}\right)\left(\sigma_H^{\wp}+\mu_H^{\wp}\right)\left(\delta_H^{\wp}+\gamma_H^{\wp}+\mu_H^{\wp}\right)}}. \tag{11}$$

From Eq. (11), it is noticed that the Ebola will increase in the community whenever the transmission rate of Ebola from humans to dogs, β_D, the transmission from dogs to humans, β_H, the recruitment rate of humans, m_1, the recruitment rate of dogs, m_2, the transfer rate of Ebola exposed humans to infectious human class, σ_H, and the transfer rate of Ebola exposed dogs to infectious dog class, σ_D increases. Furthermore, it is noticed that Ebola decreases in the community whenever the natural mortality rate of humans, μ_H, the natural mortality rate of dogs, μ_D, the Ebola-related death rate, δ_H, the recovered rate of humans, γ_H, and the recovered rate of dogs, γ_D, increases. However, the death rates cannot be used as control measures; therefore, if one chooses to control the number of secondary infections, then it is advisable to increase recovery rates in both the human and dog populations and also decrease the following: the transmission rate of Ebola from humans to dogs, β_D, the transmission from dogs to humans, β_H, the recruitment rate of humans, m_1, the recruitment rate of dogs, m_2, the transfer rate of Ebola exposed humans to infectious human class, σ_H, and the transfer rate of Ebola exposed dogs to infectious dog class, σ_D.

Theorem 3. *The Ebola-free equilibrium is locally asymptotically stable when* $R_0 < 1$ *and unstable when* $R_0 > 1$.

Existence and stability of Ebola-present equilibrium

System (3) has Ebola-present equilibrium denoted by $E_1 = (S_H^*, E_H^*, I_H^*, R_H^*, S_D^*, E_D^*, I_D^*, R_D^*)$, where

$$S_H^* = \frac{(1+\alpha_1^{\wp} I_H^*)[M_1^{\wp}(\eta_H^{\wp}+\mu_H^{\wp}) + \eta_H^{\wp}\gamma_H^{\wp} I_H^*]}{(\eta_H^{\wp}+\mu_H^{\wp})[\beta_H^{\wp} I_D^* + \mu_H^{\wp}(1+\alpha_1^{\wp} I_H^*)]}, \quad E_H^* = \frac{\beta_H^{\wp} S_H^* I_D^*}{(1+\alpha_1^{\wp} I_D^*)(\mu_H^{\wp}+\sigma_H^{\wp})},$$

$$I_H^* = \frac{\sigma_H^{\wp} E_H^*}{\gamma_H^{\wp}+\delta_H^{\wp}+\mu_H^{\wp}}, \quad R_H^* = \frac{\gamma_H^{\wp} I_H^*}{\eta_H^{\wp}+\mu_H^{\wp}}, S_D^* = \frac{[M_2^{\wp}(\eta_D^{\wp}+\mu_D^{\wp}) + \eta_D^{\wp}\gamma_D I_D^*](1+\alpha_2^{\wp} I_H^*)}{[\beta_D^{\wp} I_H^* - \mu_D^{\wp}(1+\alpha_2^{\wp} I_H)](\eta_D^{\wp}+\mu_D^{\wp})},$$

$$E_D^* = \frac{\beta_D^{\wp} S_D^* I_H^*}{(1+\alpha_2^{\wp} I_H^*)(\mu_D^{\wp}+\sigma_D^{\wp})}, \quad I_D^* = \frac{\eta_D^{\wp} E_D^*}{\gamma_D^{\wp}+\mu_D^{\wp}}, \quad R_D^* = \frac{\gamma_D^{\wp} I_D^*}{\eta_D^{\wp}+\mu_D^{\wp}}.$$

To this end, we prove the local stability of Ebola-present Equilibrium (E_1). We employ the centre manifold theorem [53] as discussed in theorem (6) of [54] and theorem (4.1) of [55] to prove the local stability of E_1.

Theorem 4. *The Ebola-present equilibrium* E_1 *of model (3) is locally asymptotically stable (LAS) if* $\mathcal{R}_0$ *is close to* 1 *[54].*

Proof. We employ the method used in theorem (4.1) of [55] to prove the local stability of E_1 by considering the transmission rate β_D as the bifurcation parameter so that $\mathcal{R}_0 = 1$ if and only if

$$\beta_D = \beta_D^{\wp *} = \frac{\mu_D^{\wp}\mu_H^{\wp}\left(\gamma_D^{\wp}+\mu_D^{\wp}\right)\left(\sigma_D^{\wp}+\mu_D^{\wp}\right)\left(\sigma_H^{\wp}+\mu_H^{\wp}\right)\left(\delta_H^{\wp}+\gamma_H^{\wp}+\mu_H^{\wp}\right)}{\beta_H^{\wp} m_1^{\wp} m_2^{\wp} \sigma_D^{\wp} \sigma_H^{\wp}}. \tag{12}$$

Considering a change in the variable, we have;

$$x = (x_1, x_2, x_3, x_4, x_5, x_6, x_7, x_8) = (S_H, E_H, I_H, R_H, S_D, E_D, I_D, R_D).$$

Consequently, total population is given by $\sum_{i=1}^{8} x_i$. Additionally, by using the vector notation for

$$x = (x_1, x_2, x_3, x_4, x_5, x_6, x_7, x_8)^T,$$

the system (3) becomes;

$$\frac{dx}{dt} = (f_1, f_2, f_3, f_4, f_5, f_6, f_7, f_8)^T.$$

The model (3) is therefore written as follows;

$$\begin{aligned}
\frac{dx_1}{dt} &= m_1^{\wp} - \frac{\beta_H^{\wp} x_1 x_7}{1+\alpha_1^{\wp} x_7} - \mu_H^{\wp} x_1 + \eta_H^{\wp} x_4 = f_1,\\
\frac{dx_2}{dt} &= \frac{\beta_H^{\wp} x_1 x_7}{1+\alpha_1^{\wp} x_7} - (\mu_H^{\wp} + \sigma_H^{\wp}) x_2 = f_2,\\
\frac{dx_3}{dt} &= \sigma_H^{\wp} x_2 - (\gamma_H^{\wp} + \delta_H^{\wp} + \mu_H^{\wp}) x_3 = f_3,\\
\frac{dx_4}{dt} &= \gamma_H^{\wp} x_3 - (\eta_H^{\wp} + \mu_H^{\wp}) x_4 = f_4,\\
\frac{dx_5}{dt} &= m_2^{\wp} - \frac{\beta_D^{\wp} x_5 x_3}{1+\alpha_2^{\wp} x_3} - \mu_D^{\wp} x_5 + \eta_D^{\wp} x_8 = f_5,\\
\frac{dx_6}{dt} &= \frac{\beta_D^{\wp} x_5 x_3}{1+\alpha_2^{\wp} x_3} - (\sigma_D^{\wp} + \mu_D^{\wp}) x_6 = f_6,\\
\frac{dx_7}{dt} &= \sigma_D^{\wp} x_6 - (\gamma_D^{\wp} + \mu_D^{\wp}) x_7 = f_7,\\
\frac{dx_7}{dt} &= \gamma_D x_7 - (\eta_D^{\wp} + \mu_D^{\wp}) x_8 = f_8.
\end{aligned} \tag{13}$$

Model System (13) evaluated at E^0 gives the Jacobian matrix, denoted by $J(E_*^0)$. It is therefore given by

$$J(E_*^0) = \begin{pmatrix}
-\mu_H^{\wp} & 0 & 0 & \eta_H^{\wp} & 0 & 0 & -\beta_H^{\wp} x_1 & 0\\
0 & -(\mu_H^{\wp} + \sigma_H^{\wp}) & 0 & 0 & 0 & 0 & \beta_H^{\wp} x_1 & 0\\
0 & \sigma_H^{\wp} & -(\gamma_H^{\wp} + \delta_H^{\wp} + \mu_H^{\wp}) & 0 & 0 & 0 & 0 & 0\\
0 & 0 & \gamma_H^{\wp} & -(\eta_H^{\wp} + \mu_H^{\wp}) & 0 & 0 & 0 & 0\\
0 & 0 & -\beta_D^{\wp} x_5 & 0 & -\mu_D^{\wp} & 0 & 0 & \eta_D^{\wp}\\
0 & 0 & \beta_D^{\wp} x_5 & 0 & 0 & -(\mu_D^{\wp} + \sigma_D^{\wp}) & 0 & 0\\
0 & 0 & 0 & 0 & 0 & \sigma_D^{\wp} & -(\gamma_D^{\wp} + \mu_D^{\wp}) & 0\\
0 & 0 & 0 & 0 & 0 & 0 & \gamma_D^{\wp} & -(\eta_D^{\wp} + \mu_D^{\wp})
\end{pmatrix}.$$

Let,

$$z_1 = (\mu_H^{\wp} + \sigma_H^{\wp}), z_2 = (\gamma_H^{\wp} + \delta_H^{\wp} + \mu_H^{\wp}), z_3 = (\eta_H^{\wp} + \mu_H^{\wp}), z_4 = (\mu_D^{\wp} + \sigma_D^{\wp}), z_5 = (\gamma_D^{\wp} + \mu_D^{\wp}), z_6 = (\eta_D^{\wp} + \mu_D^{\wp}),$$

so that $J(E_*^0)$ becomes

$$J(E_*^0) = \begin{pmatrix}
-\mu_H^{\wp} & 0 & 0 & \eta_H^{\wp} & 0 & 0 & -\beta_H^{\wp} x_1 & 0\\
0 & -z_1 & 0 & 0 & 0 & 0 & \beta_H^{\wp} x_1 & 0\\
0 & \sigma_H^{\wp} & -z_2 & 0 & 0 & 0 & 0 & 0\\
0 & 0 & \gamma_H^{\wp} & -z_3 & 0 & 0 & 0 & 0\\
0 & 0 & -\beta_D^{\wp} x_5 & 0 & -\mu_D^{\wp} & 0 & 0 & \eta_D^{\wp}\\
0 & 0 & \beta_D^{\wp} x_5 & 0 & 0 & -z_4 & 0 & 0\\
0 & 0 & 0 & 0 & 0 & \sigma_D^{\wp} & -z_5 & 0\\
0 & 0 & 0 & 0 & 0 & 0 & \gamma_D^{\wp} & -z_6
\end{pmatrix}. \tag{14}$$

Solving for the eigenvalues of matrix (14). We noticed that the Jacobian matrix (14) has a simple eigenvalue, with other eigenvalues having negative real parts. Hence, the centre manifold theorem [55] can be applied. We therefore need to compute **a** and **b** given by

$$\mathbf{a} = \sum_{k,i=1}^{n} \frac{v_k w_i w_j \delta^2 f_k(0,0)}{\delta x_i \delta x_j},$$

and

$$\mathbf{b} = \sum_{k,i=1}^{n} \frac{v_k w_i \delta^2 f_k(0,0)}{\delta x_i \delta \beta_D^{\wp}}.$$

Also, the right and left eigenvectors are computed in that order and are represented by;

$$W = [w_1, w_2, w_3, w_4, w_5, w_6, w_7, w_8]^T, \text{and}, V = [v_1, v_2, v_3, v_4, v_5, v_6, v_7, v_8].$$

We obtained;

$$J(E_*^0)=\begin{pmatrix} -\mu_H^{\wp} & 0 & 0 & \eta_H^{\wp} & 0 & 0 & -\beta_H^{\wp}x_1 & 0\\ 0 & -z & 0 & 0 & 0 & 0 & \beta_H^{\wp}x_1 & 0\\ 0 & \sigma_H^{\wp} & -z_2 & 0 & 0 & 0 & 0 & 0\\ 0 & 0 & \gamma_H & -z_3 & 0 & 0 & 0 & 0\\ 0 & 0 & -\beta_D^{\wp}x_5 & 0 & -\mu_D & 0 & 0 & \eta_D\\ 0 & 0 & \beta_D^{\wp}x_5 & 0 & 0 & -z_4 & 0 & 0\\ 0 & 0 & 0 & 0 & 0 & \sigma_D^{\wp} & -z_5 & 0\\ 0 & 0 & 0 & 0 & 0 & 0 & \gamma_D^{\wp} & -z_6 \end{pmatrix}\begin{pmatrix} w_1\\ w_2\\ w_3\\ w_4\\ w_5\\ w_6\\ w_7\\ w_8 \end{pmatrix}=\begin{pmatrix} 0\\ 0\\ 0\\ 0\\ 0\\ 0\\ 0\\ 0 \end{pmatrix}. \tag{15}$$

From Eq. (15), the right-eigenvectors are obtained as;

$$w_1=\frac{(z_4z_5\eta_H^{\wp}\gamma_H^{\wp}-z_3\beta_H^{\wp}x_1\sigma_D^{\wp}x_5)w_3}{z_3z_4z_5\mu_H^{\wp}}, w_2=\frac{z_2w_3}{\sigma_H^{\wp}}, w_3=1, w_4=\frac{\gamma_H^{\wp}w_3}{z_3},$$
$$w_5=\frac{(\eta_D^{\wp}\gamma_D^{\wp}\sigma_D^{\wp}-z_4z_5z_6)\beta_D^{\wp}x_5w_3}{z_4z_5z_6\mu_D^{\wp}}, w_6=\frac{\beta_D^{\wp}x_5w_3}{z_4}, w_7=\frac{\sigma_D^{\wp}\beta_D^{\wp}x_5w_3}{z_4z_5},$$
$$w_8=\frac{\gamma_D^{\wp}\sigma_D^{\wp}\beta_D^{\wp}x_5w_3}{z_4z_5z_6}.$$

Similarly, the left eigenvectors are computed as follows:

$$J(E_*^0)=\mathcal{H}\begin{pmatrix} -\mu_H^{\wp} & 0 & 0 & \eta_H^{\wp} & 0 & 0 & -\beta_H^{\wp}x_1 & 0\\ 0 & -z_1 & 0 & 0 & 0 & 0 & \beta_H^{\wp}x_1 & 0\\ 0 & \sigma_H^{\wp} & -z_2 & 0 & 0 & 0 & 0 & 0\\ 0 & 0 & -\gamma_H^{\wp} & -z_3 & 0 & 0 & 0 & 0\\ 0 & 0 & -\beta_D^{\wp}x_5 & 0 & -\mu_D^{\wp} & 0 & 0 & \eta_D^{\wp}\\ 0 & 0 & \beta_D^{\wp}x_5 & 0 & 0 & -z_4 & 0 & 0\\ 0 & 0 & 0 & 0 & 0 & \sigma_D^{\wp} & -z_5 & 0\\ 0 & 0 & 0 & 0 & 0 & 0 & \gamma_D^{\wp} & -z_6 \end{pmatrix}=\begin{pmatrix} 0\\ 0\\ 0\\ 0\\ 0\\ 0\\ 0\\ 0 \end{pmatrix}, \tag{16}$$

where, $\mathcal{H}=(v_1,v_2,v_3,v_4,v_5,v_6,v_7,v_8)$, thus, solving the above Eq. (16), we obtain, the following;

$$v_1=v_4=v_8=v_5=0, v_3=1, v_2=\frac{\sigma_H^{\wp}v_3}{z_1}, v_6=\frac{\sigma_D^{\wp}\beta_H^{\wp}x_1\sigma_H^{\wp}v_3}{z_1z_4z_5}, v_7=\frac{\beta_H^{\wp}x_1\sigma_H^{\wp}v_3}{Z_1z_5}.$$

The non-zero partial derivatives at the Ebola-free equilibrium E_0 are given by

$$\frac{\partial^2 f_1}{\partial x_7\partial x_1}=-\beta_H^{\wp}, \quad \frac{\partial^2 f_2}{\partial x_7\partial x_1}=\beta_H^{\wp}, \quad \frac{\partial^2 f_5}{\partial x_3\partial x_5}=-\beta_D^{\wp}, \quad \frac{\partial^2 f_6}{\partial x_3\partial x_5}=\beta_D^{\wp}, \quad \frac{\partial^2 f_6}{\partial x_3\partial\beta_D^{\wp}}=\frac{M_2}{\beta_D^{\wp}}.$$

From the calculations performed, the values for **a** and **b** are given as:

$$\mathbf{a}=\frac{2\sigma_H^{\wp}\sigma_D^{\wp}\beta_H^{\wp}\beta_DM_2}{(\mu_H^{\wp}+\sigma_H^{\wp})(\mu_D^{\wp}+\sigma_D^{\wp})(\gamma_D^{\wp}+\mu_D^{\wp})\mu_D^{\wp}}\left[\mathcal{G}_1+M_1\mathcal{G}_2\right],$$
$$\mathbf{b}=\frac{M_1^{\wp}M_2^{\wp}\sigma_H^{\wp}\sigma_D^{\wp}\beta_H^{\wp}v_3}{\mu_D\mu_H^{\wp}}.$$

Where $\mathcal{G}_1=\frac{(\mu_D^{\wp}+\sigma_D^{\wp})(\gamma_D^{\wp}+\mu_D^{\wp})\eta_H^{\wp}\gamma_H^{\wp}-(\eta_H^{\wp}+\mu_H^{\wp})\beta_H^{\wp}\beta_D\sigma_D^{\wp}M_1^{\wp}M_2^{\wp}}{(\eta_H^{\wp}+\mu_H^{\wp})(\mu_D^{\wp}+\sigma_D^{\wp})(\gamma_D^{\wp}+\mu_D^{\wp})(\mu_H^{\wp})^2\mu_D^{\wp}}$, and $\mathcal{G}_2=\frac{(\eta_D^{\wp}\gamma_D^{\wp}\sigma_D^{\wp}-(\mu_D^{\wp}+\sigma_D^{\wp})(\gamma_D^{\wp}+\mu_D^{\wp})(\eta_D^{\wp}+\mu_D^{\wp}))}{(\mu_D^{\wp}+\sigma_D^{\wp})(\gamma_D^{\wp}+\mu_D^{\wp})(\eta_D^{\wp}+\mu_D^{\wp})\mu_H^{\wp}\mu_D^{\wp}}$. It can be seen that the computation of **b** is positive. The sign of the coefficients of **a** and **b** determines the local dynamics around the Ebola-free equilibrium for β_D^*. It follows from the results given by [55–57], that model (3) undergoes backward bifurcation if

$$(\mu_D^{\wp}+\gamma_D^{\wp})(\gamma_D^{\wp}+\mu_D^{\wp})\eta_H^{\wp}\gamma_H^{\wp}>(\eta_H^{\wp}+\mu_H^{\wp})\beta_H^{\wp}\beta_D^{\wp}\sigma_D^{\wp}M_1^{\wp}M_2^{\wp}, \text{and } \eta_D^{\wp}\gamma_D^{\wp}\sigma_D^{\wp}>(\mu_D^{\wp}+\sigma_D^{\wp})(\gamma_D^{\wp}+\mu_D^{\wp})(\eta_D^{\wp}+\mu_D^{\wp}),$$

so that $\mathbf{a}>0$ and $\mathbf{b}>0$. Also, model d undergoes a forward bifurcation if

$$(\mu_D^{\wp}+\gamma_D^{\wp})(\gamma_D^{\wp}+\mu_D^{\wp})\eta_H^{\wp}\gamma_H^{\wp}<(\eta_H^{\wp}+\mu_H^{\wp})\beta_H^{\wp}\beta_D^{\wp}\sigma_D^{\wp}M_1^{\wp}M_2^{\wp}, \text{and } \eta_D^{\wp}\gamma_D^{\wp}\sigma_D^{\wp}<(\mu_D^{\wp}+\sigma_D^{\wp})(\gamma_D^{\wp}+\mu_D^{\wp})(\eta_D^{\wp}+\mu_D^{\wp}),$$

so that $\mathbf{a}<0$ and $\mathbf{b}>0$. According to our analysis above, it can be seen that $\mathcal{R}_0<1$, can guarantee the global stability of the Ebola-free equilibrium. The presence of forward bifurcation shows that Ebola can be eliminated by decreasing the $\mathcal{R}_0$ to a value less than unity, which is numerically shown in Section "Parameter estimation and numerical simulations", Fig. 3.

Existence and uniqueness of the proposed model

Now, by considering Eq. (2), the fractional order derivative of the Ebola model in the sense of Caputo–Fabrizio, we establish the existence of solutions of the model (2) through the use of the Picard–Lindelof approach. We, thus, convert the Ebola model (2) in the form of a fractional integral. This is done by applying the Caputo–Fabrizio integral operator as defined in (1) to the model (2). By considering the following initial values of the state variables; $S_H(0) = S_H^0, E_H(0) = E_H^0, I_H(0) = I_H^0, R_H(0) = R_H^0, S_D(0) = S_D^0, E_D(0) = E_D^0, I_D(0) = I_D^0$ and $R_D(0) = R_D^0$, yields;

$$
\begin{aligned}
S_H(t) &= S_{H0} + \frac{2(1-\wp)}{(2-\wp)\mathfrak{V}(\wp)}\left[m_1^\wp - \frac{\beta_H^\wp S_H I_D}{1+\alpha_1 I_D} - \mu_H^\wp S_H + \eta_H^\wp R_H\right] + \frac{2\wp}{(2-\wp)\mathfrak{V}(\wp)}\int_0^t \left[m_1^\wp - \frac{\beta_H^\wp S_H I_D}{1+\alpha_1 I_D} - \mu_H^\wp S_H + \eta_H^\wp R_H\right] d\tau,\\
E_H(t) &= E_{H0} + \frac{2(1-\wp)}{(2-\wp)\mathfrak{V}(\wp)}\left[\frac{\beta_H^\wp S_H I_D}{1+\alpha_1 I_D} - (\mu_H^\wp + \sigma_H^\wp)E_H\right] + \frac{2\wp}{(2-\wp)\mathfrak{V}(\wp)}\int_0^t \left[\frac{\beta_H^\wp S_H I_D}{1+\alpha_1 I_D} - (\mu_H^\wp + \sigma_H^\wp)E_H\right] d\tau,\\
I_H(t) &= I_{H0} + \frac{2(1-\wp)}{(2-\wp)\mathfrak{V}(\wp)}(\sigma_H^\wp E_H - (\gamma_H^\wp + \delta_H^\wp + \mu_H^\wp)I_H) + \frac{2\wp}{(2-\wp)\mathfrak{V}(\wp)}\int_0^t (\sigma_H^\wp E_H - (\gamma_H^\wp + \delta_H^\wp + \mu_H^\wp)I_H) d\tau,\\
R_H(t) &= R_{H0} + \frac{2(1-\wp)}{(2-\wp)\mathfrak{V}(\wp)}(\gamma_H^\wp I_H - (\eta_H + \mu_H^\wp)R_H) + \frac{2\wp}{(2-\wp)\mathfrak{V}(\wp)}\int_0^t (\gamma_H^\wp I_H - (\eta_H^\wp + \mu_H^\wp)R_H) d\tau,\\
S_D(t) &= S_{D0} + \frac{2(1-\wp)}{(2-\wp)\mathfrak{V}(\wp)}\left[m_2^\wp - \frac{\beta_D^\wp S_D I_H}{1+\alpha_2 I_H} - \mu_D^\wp S_D + \eta_D^\wp R_D\right] + \frac{2\wp}{(2-\wp)\mathfrak{V}(\wp)}\int_0^t \left[m_2^\wp - \frac{\beta_D^\wp S_D I_H}{1+\alpha_2 I_H} - \mu_D^\wp S_D + \eta_D^\wp R_D\right] d\tau,\\
E_D(t) &= E_{D0} + \frac{2(1-\wp)}{(2-\wp)\mathfrak{V}(\wp)}\left[\frac{\beta_D^\wp S_D I_H}{1+\alpha_2 I_H} - (\sigma_D^\wp + \mu_D^\wp)E_D\right] + \frac{2\wp}{(2-\wp)\mathfrak{V}(\wp)}\int_0^t \left[\frac{\beta_D^\wp S_D I_H}{1+\alpha_2 I_H} - (\sigma_D^\wp + \mu_D^\wp)E_D\right] d\tau,\\
I_D(t) &= I_{D0} + \frac{2(1-\wp)}{(2-\wp)\mathfrak{V}(\wp)}(\sigma_D^\wp E_D - (\gamma_D^\wp + \mu_D^\wp)I_D) + \frac{2\wp}{(2-\wp)\mathfrak{V}(\wp)}\int_0^t (\sigma_D^\wp E_D - (\gamma_D^\wp + \mu_D^\wp)I_D) d\tau,\\
R_D(t) &= R_{D0} + \frac{2(1-\wp)}{(2-\wp)\mathfrak{V}(\wp)}(\gamma_D^\wp I_D - (\eta_D^\wp + \mu_D^\wp)R_D) + \frac{2\wp}{(2-\wp)\mathfrak{V}(\wp)}\int_0^t (\gamma_D^\wp I_D - (\eta_D^\wp + \mu_D^\wp)R_D) d\tau.
\end{aligned}
\tag{17}
$$

We then apply the Picard iterative algorithm in this manner as $i = 0, 1, 2, \ldots$

$S_H(0) = S_H^0, E_H(0) = E_H^0, I_H(0) = I_H^0, R_H(0) = R_H^0, S_D(0) = S_D^0, E_D(0) = E_D^0, I_D(0) = I_D^0, R_D(0) = R_D^0$ and,

$$
\begin{aligned}
S_{H\,i+1}(t) &= S_{H0} + \frac{2(1-\wp)}{(2-\wp)\mathfrak{V}(\wp)}\left[m_1^\wp - \frac{\beta_H^\wp S_H I_D}{1+\alpha_1 I_D} - \mu_H^\wp S_H + \eta_H^\wp R_H\right]\\
&\quad + \frac{2\wp}{(2-\wp)\mathfrak{V}(\wp)}\int_0^t \left[m_1^\wp - \frac{\beta_H^\wp S_H I_D}{1+\alpha_1 I_D} - \mu_H^\wp S_H + \eta_H^\wp R_H\right] d\tau,\\
E_{H\,i+1}(t) &= E_{H0} + \frac{2(1-\wp)}{(2-\wp)\mathfrak{V}(\wp)}\left[\frac{\beta_H^\wp S_H I_D}{1+\alpha_1 I_D} - (\mu_H^\wp + \sigma_H^\wp)E_H\right] + \frac{2\wp}{(2-\wp)\mathfrak{V}(\wp)}\int_0^t \left[\frac{\beta_H^\wp S_H I_D}{1+\alpha_1 I_D} - (\mu_H^\wp + \sigma_H^\wp)E_H\right] d\tau,\\
I_{H\,i+1}(t) &= I_{H0} + \frac{2(1-\wp)}{(2-\wp)\mathfrak{V}(\wp)}(\sigma_H^\wp E_H - (\gamma_H^\wp + \delta_H^\wp + \mu_H^\wp)I_H) + \frac{2\wp}{(2-\wp)\mathfrak{V}(\wp)}\int_0^t (\sigma_H^\wp E_H - (\gamma_H^\wp + \delta_H^\wp + \mu_H^\wp)I_H) d\tau,\\
R_{H\,i+1}(t) &= R_{H0} + \frac{2(1-\wp)}{(2-\wp)\mathfrak{V}(\wp)}(\gamma_H^\wp I_H - (\eta_H^\wp + \mu_H^\wp)R_H) + \frac{2\wp}{(2-\wp)\mathfrak{V}(\wp)}\int_0^t (\gamma_H^\wp I_H - (\eta_H + \mu_H^\wp)R_H) d\tau,\\
S_{D\,i+1}(t) &= S_{D0} + \frac{2(1-\wp)}{(2-\wp)\mathfrak{V}(\wp)}\left[m_2^\wp - \frac{\beta_D^\wp S_D I_H}{1+\alpha_2 I_H} - \mu_D^\wp S_D + \eta_D^\wp R_D\right]\\
&\quad + \frac{2\wp}{(2-\wp)\mathfrak{V}(\wp)}\int_0^t \left[m_2^\wp - \frac{\beta_D^\wp S_D I_H}{1+\alpha_2 I_H} - \mu_D^\wp S_D + \eta_D^\wp R_D\right] d\tau,\\
E_{D\,i+1}(t) &= E_{D0} + \frac{2(1-\wp)}{(2-\wp)\mathfrak{V}(\wp)}\left[\frac{\beta_D^\wp S_D I_H}{1+\alpha_2 I_H} - (\sigma_D^\wp + \mu_D^\wp)E_D\right] + \frac{2\wp}{(2-\wp)\mathfrak{V}(\wp)}\int_0^t \left[\frac{\beta_D^\wp S_D I_H}{1+\alpha_2 I_H} - (\sigma_D^\wp + \mu_D^\wp)E_D\right] d\tau,\\
I_{D\,i+1}(t) &= I_{D0} + \frac{2(1-\wp)}{(2-\wp)\mathfrak{V}(\wp)}(\sigma_D^\wp E_D - (\gamma_D^\wp + \mu_D^\wp)I_D) + \frac{2\wp}{(2-\wp)\mathfrak{V}(\wp)}\int_0^t (\sigma_D^\wp E_D - (\gamma_D^\wp + \mu_D^\wp)I_D) d\tau,\\
R_{D\,i+1}(t) &= R_{D0} + \frac{2(1-\wp)}{(2-\wp)\mathfrak{V}(\wp)}(\gamma_D^\wp I_D - (\eta_D^\wp + \mu_D^\wp)R_D) + \frac{2\wp}{(2-\wp)\mathfrak{V}(\wp)}\int_0^t (\gamma_D^\wp I_D - (\eta_D^\wp + \mu_D^\wp)R_D) d\tau.
\end{aligned}
\tag{18}
$$

By assuming that there exists a true value to the fractional Ebola model (2), we take the limits of Eq. (18) as $i \longrightarrow \infty$. We obtain the solution;

$$
\begin{aligned}
&\lim_{i\longrightarrow\infty} S_{H\,i}(t) = S_H(t),\ \lim_{i\longrightarrow\infty} E_{H\,i}(t) = E_H(t),\ \lim_{i\longrightarrow\infty} I_{H\,i}(t) = I_H(t),\ \lim_{i\longrightarrow\infty} R_{H\,i}(t) = R_H(t),\\
&\lim_{i\longrightarrow\infty} S_{D\,i}(t) = S_D(t),\ \lim_{i\longrightarrow\infty} E_{D\,i}(t) = S_E(t),\ \lim_{i\longrightarrow\infty} I_{D\,i}(t) = I_D(t),\ \lim_{i\longrightarrow\infty} R_{D\,i}(t) = R_D(t).
\end{aligned}
\tag{19}
$$

To demonstrate the existence of a solution to the Ebola model (2) with fractional operators and to meet the uniqueness requirement using the Picard–Lindelof technique, the following transformations are defined:

$$\begin{aligned}
\mathfrak{F}_1(t,S_H) &= m_1^{\wp} - \frac{\beta_H^{\wp} S_H I_D}{1+\alpha_1 I_D} - \mu_H^{\wp} S_H + \eta_H^{\wp} R_H,\\
\mathfrak{F}_2(t,E_H) &= \frac{\beta_H^{\wp} S_H I_D}{1+\alpha_1 I_D} - (\mu_H^{\wp} + \sigma_H^{\wp}) E_H,\\
\mathfrak{F}_3(t,I_H) &= \sigma_H^{\wp} E_H - (\gamma_H^{\wp} + \delta_H^{\wp} + \mu_H^{\wp}) I_H,\\
\mathfrak{F}_4(t,R_H) &= \gamma_H^{\wp} I_H - (\eta_H^{\wp} + \mu_H^{\wp}) R_H,\\
\mathfrak{F}_5(t,S_D) &= m_2^{\wp} - \frac{\beta_D^{\wp} S_D I_H}{1+\alpha_2 I_H} - \mu_D^{\wp} S_D + \eta_D^{\wp} R_D,\\
\mathfrak{F}_6(t,E_D) &= \frac{\beta_D^{\wp} S_D I_H}{1+\alpha_2 I_H} - (\sigma_D^{\wp} + \mu_D^{\wp}) E_D,\\
\mathfrak{F}_7(t,I_D) &= \sigma_D^{\wp} E_D - (\mu_D^{\wp} + \gamma_D^{\wp}) I_D,\\
\mathfrak{F}_8(t,R_D) &= \gamma_D^{\wp} I_D - (\eta_D^{\wp} + \mu_D^{\wp}) R_D.
\end{aligned} \tag{20}$$

where the transformations $\mathfrak{F}(t,S_H), \mathfrak{F}(t,E_H), \mathfrak{F}(t,I_H), \mathfrak{F}(t,R_H), \mathfrak{F}(t,S_D), \mathfrak{F}(t,E_D), \mathfrak{F}(t,I_D)$ and $\mathfrak{F}(t,R_D)$ are contractions with respect to the functions. By further considering the following cartesian products;

$$\begin{aligned}
\mathcal{M}_{\alpha,\beta_1} &:= [t-\alpha, t+\alpha] \times [S_H - \beta_1, S_H + \beta_1] = U \times V_1,\\
\mathcal{M}_{\alpha,\beta_2} &:= [t-\alpha, t+\alpha] \times [E_H - \beta_1, E_H + \beta_1] = U \times V_2,\\
\mathcal{M}_{\alpha,\beta_3} &:= [t-\alpha, t+\alpha] \times [I_H - \beta_1, I_H + \beta_1] = U \times V_3,\\
\mathcal{M}_{\alpha,\beta_4} &:= [t-\alpha, t+\alpha] \times [R_H - \beta_1, R_H + \beta_1] = U \times V_4,\\
\mathcal{M}_{\alpha,\beta_5} &:= [t-\alpha, t+\alpha] \times [S_D - \beta_1, S_H + \beta_1] = U \times V_5,\\
\mathcal{M}_{\alpha,\beta_6} &:= [t-\alpha, t+\alpha] \times [E_D - \beta_1, E_H + \beta_1] = U \times V_6,\\
\mathcal{M}_{\alpha,\beta_7} &:= [t-\alpha, t+\alpha] \times [I_D - \beta_1, I_H + \beta_1] = U \times V_7,\\
\mathcal{M}_{\alpha,\beta_8} &:= [t-\alpha, t+\alpha] \times [R_D - \beta_1, R_H + \beta_1] = U \times V_8.
\end{aligned} \tag{21}$$

By taking

$$\mathfrak{F}_1^* \sup_{(t,S_H)\in\mathfrak{I}} \|\mathfrak{F}_1(t,S_H(t))\|,\ \mathfrak{F}_2^* \sup_{(t,E_H)\in\mathfrak{I}} \|\mathfrak{F}_1(t,E_H(t))\|,\ \mathfrak{F}_3^* \sup_{(t,I_H)\in\mathfrak{I}} \|\mathfrak{F}_1(t,I_H(t))\|,\ \mathfrak{F}_4^* \sup_{(t,R_H)\in\mathfrak{I}} \|\mathfrak{F}_1(t,R_H(t))\|,$$
$$\mathfrak{F}_5^* \sup_{(t,S_D)\in\mathfrak{I}} \|\mathfrak{F}_1(t,S_D(t))\|,\ \mathfrak{F}_6^* \sup_{(t,E_D)\in\mathfrak{I}} \|\mathfrak{F}_1(t,E_D(t))\|,\ \mathfrak{F}_7^* \sup_{(t,I_D)\in\mathfrak{I}} \|\mathfrak{F}_1(t,I_D(t))\|,\ \mathfrak{F}_8^* \sup_{(t,R_D)\in\mathfrak{I}} \|\mathfrak{F}_1(t,R_D(t))\|.$$

With the above information, we therefore state the Picard transformation as

$$\aleph : \mathcal{C}(U,\mathcal{P}_1,\mathcal{P}_2,\mathcal{P}_3,\mathcal{P}_4,\mathcal{P}_5,\mathcal{P}_6,\mathcal{P}_7,\mathcal{P}_8) \longrightarrow \mathcal{C}(U,\mathcal{P}_1,\mathcal{P}_2,\mathcal{P}_3,\mathcal{P}_4,\mathcal{P}_5,\mathcal{P}_6,\mathcal{P}_7,\mathcal{P}_8).$$

In this manner, we express

$$\aleph(\mathbb{Q}(t)) = \mathbb{Q}_0(t) + \frac{2(1-\wp)}{(2-\wp)\mathfrak{V}(\wp)}\mathcal{B}(t,\mathbb{Q}(t)) + \frac{2\wp}{(2-\wp)\mathfrak{V}(\wp)}\int_0^t \mathcal{B}(t,\mathbb{Q}(t))d\tau. \tag{22}$$

Where $\mathbb{Q}(t) = S_H(t), E_H(t), I_H(t), R_H(t), S_D(t), E_D(t), I_D(t), R_D(t)$, $\mathbb{Q}_0(t) = (S_{H0}, E_{H0}, I_{H0}, R_{H0}, S_{D0}, E_{D0}, I_{D0}, R_{D0})$ and $\mathcal{B}(t,\mathbb{Q}) = \mathfrak{F}_1(t,S_H), \mathfrak{F}_2(t,S_H), \mathfrak{F}_3(t,S_H), \mathfrak{F}_4(t,S_H), \mathfrak{F}_5(t,S_H), \mathfrak{F}_6(t,S_H), \mathfrak{F}_7(t,S_H), \mathfrak{F}_8(t,S_H)$. We proceed by defining a norm on the space $\mathcal{C}(U,\mathcal{P}_1,\mathcal{P}_2,\mathcal{P}_3,\mathcal{P}_4,\mathcal{P}_5,\mathcal{P}_6,\mathcal{P}_7,\mathcal{P}_8)$ so as to apply the Picard theorem as $\|\mathbb{Q}\|_\infty = \sup_{t\in[t-\alpha,t+\alpha]=U} |\mathbb{Q}(t)|$. We further assume that the boundedness condition is satisfied by solutions within the time interval, thus;

$$\|\mathbb{Q}\|_\infty \le \max\{\beta_1,\beta_2,\beta_3,\beta_4,\beta_5,\beta_6,\beta_7,\beta_8\} = b.$$

Again, we assume that $\mathcal{M}^{\circledast} = \max\{\mathcal{M}_1^{\circledast}, \mathcal{M}_2^{\circledast}, \mathcal{M}_3^{\circledast}, \mathcal{M}_4^{\circledast}, \mathcal{M}_5^{\circledast}, \mathcal{M}_6^{\circledast}, \mathcal{M}_7^{\circledast}, \mathcal{M}_8^{\circledast}\}$ and there exists t_0 with $t \le t_0$. This yields;

$$\begin{aligned}
\|\aleph(\mathbb{Q}(t)) - \mathbb{Q}_0(t)\| &= \left\| \frac{2(1-\wp)}{(2-\wp)\mathfrak{V}(\wp)}\mathcal{B}(t,\mathbb{Q}(t)) + \frac{2\wp}{(2-\wp)\mathfrak{V}(\wp)}\int_0^t \mathcal{B}(\tau,\mathbb{Q}(\tau)) \right\| d\tau,\\
&\le \frac{2(1-\wp)}{(2-\wp)\mathfrak{V}(\wp)}\|\mathcal{B}(t,\mathbb{Q}(t))\| + \frac{2\wp}{(2-\wp)\mathfrak{V}(\wp)}\int_0^t \|\mathcal{B}(\tau,\mathbb{Q}(\tau))\| d\tau,\\
&\le \left[\frac{2(1-\wp)}{(2-\wp)\mathfrak{V}(\wp)} + \frac{2\wp t_0}{(2-\wp)\mathfrak{V}(\wp)}\right]\mathcal{M}^{\circledast},\\
&= \Phi^{\circledast}\aleph^{\circledast},\\
&\le b.
\end{aligned} \tag{23}$$

where $\Phi^{\circledast} < \frac{b}{\aleph}$ and $\Phi^{\circledast} = \frac{2(1-\wp)}{(2-\wp)\mho(\wp)} + \frac{2\wp t_0}{(2-\wp)\mho(\wp)}$. We then show that the Picard operator $\aleph$ suffices a contraction. We have already established that the following transformations $\mathcal{M}_1^*, \mathcal{M}_2^*, \mathcal{M}_3^*, \mathcal{M}_4^*, \mathcal{M}_5^*, \mathcal{M}_6^*, \mathcal{M}_7^*, \mathcal{M}_8^*$ are contractions for every $\mathbb{Q}_1, \mathbb{Q}_2 \in C(U, \mathcal{P}_1, \mathcal{P}_2, \mathcal{P}_3, \mathcal{P}_4, \mathcal{P}_5, \mathcal{P}_6, \mathcal{P}_7, \mathcal{P}_8)$, thus, we obtain;

$$\|\mathcal{B}(t, \mathbb{Q}_1(t)) - \mathcal{B}(t, \mathbb{Q}_2(t))\| \leq \omega^{\circledast} \|\mathbb{Q}_1(t) - \mathbb{Q}_2(t)\|, \tag{24}$$

given that $\omega^{\circledast}$ is the contraction constant. By applying the Picard operator $\aleph$ definition in Eq. (22), the inequality (24) and the equality

$$\|\aleph\mathbb{Q}_1 - \aleph\mathbb{Q}_2\| = \sup_{t\in U} |\mathbb{Q}_1(t) - \mathbb{Q}_2(t)|, \tag{25}$$

this suffices that

$$\begin{aligned}
\|\aleph(\mathbb{Q}_1(t)) - \aleph\mathbb{Q}_2(t)\| &= \left\| \frac{2(1-\wp)}{(2-\wp)\mho(\wp)} [\mathcal{B}(t, \mathbb{Q}_1(t)) - \mathcal{B}(t, \mathbb{Q}_2(t))] + \frac{2\wp}{(2-\wp)\mho(\wp)} \int_0^t [\mathcal{B}(t, \mathbb{Q}_1(t)) - \mathcal{B}(t, \mathbb{Q}_2(t))] \right\| d\tau, \\
&\leq \frac{2(1-\wp)\omega^*}{(2-\wp)\mho(\wp)} \|\mathbb{Q}_1(t) - \mathbb{Q}_2(t)\| + \frac{2\wp\,\omega^{\circledast}}{(2-\wp)\mho(\wp)} \int_0^t \|\mathbb{Q}_1(\tau) - \mathbb{Q}_2(\tau)\| d\tau, \\
&\leq \left[\frac{2(1-\wp)}{(2-\wp)\mho(\wp)} + \frac{2\wp t_0}{(2-\wp)\mho(\wp)} \right] \omega^{\circledast} \|\mathbb{Q}_1(t) - \mathbb{Q}_2(t)\|, \\
&= \Phi^{\circledast}\omega^{\circledast} \|\mathbb{Q}_1(t) - \mathbb{Q}_2(t)\|.
\end{aligned} \tag{26}$$

This, therefore, posits that

$$\|\aleph\mathbb{Q}_1 - \aleph\mathbb{Q}_2\|_\infty \leq \Phi^{\circledast}\omega^{\circledast} \|\mathbb{Q}_1(t) - \mathbb{Q}_2(t)\|_\infty. \tag{27}$$

The sufficiency condition for the transformation $\aleph$ to be a contraction is that the constant $\Phi^{\circledast}\omega^{\circledast}$ be less than 1, given that $\omega^{\circledast}$ is less than 1. Hence, applying the Banach fixed point theorem allows us to conclude that the fractional model for Ebola, as represented by (2), produces a unique outcome.

Sumudu transform stability criterion

The stability of the Ebola model (2) with fractional operators is established by a recursive approach utilising the Sumudu transform technique. The data is acquired;

$$\begin{aligned}
\mathcal{ST}[{}^{CF}D_0^{\wp} S_H(t)](s) &= \mathcal{ST}\left[m_1^{\wp} - \frac{\beta_H^{\wp} S_H I_D}{1+\alpha_1 I_D} - \mu_H^{\wp} S_H + \eta^{\wp} R_H \right](s), \\
\mathcal{ST}[{}^{CF}D_0^{\wp} E_H(t)](s) &= \mathcal{ST}\left[\frac{\beta_H^{\wp} S_H I_D}{1+\alpha_1 I_D} - (\mu_H^{\wp} + \sigma_H^{\wp}) E_H \right](s), \\
\mathcal{ST}[{}^{CF}D_0^{\wp} I_H(t)](s) &= \mathcal{ST}[\sigma_H^{\wp} E_H - (\gamma_H^{\wp} + \delta_H^{\wp} + \mu_H^{\wp}) I_H](s), \\
\mathcal{ST}[{}^{CF}D_0^{\wp} R_H(t)](s) &= [\gamma_H^{\wp} I_H - (\eta_H^{\wp} + \mu_H^{\wp}) R_H](s), \\
\mathcal{ST}[{}^{CF}D_0^{\wp} S_D(t)](s) &= \mathcal{ST}\left[m_2^{\wp} - \frac{\beta_D^{\wp} S_D I_H}{1+\alpha_2 I_H} - \mu_D^{\wp} S_D + \eta_D^{\wp} R_D \right](s), \\
\mathcal{ST}[{}^{CF}D_0^{\wp} E_D(t)](s) &= \left[\frac{\beta_D^{\wp} S_D I_H}{1+\alpha_2 I_H} - (\sigma_D^{\wp} + \mu_D^{\wp}) E_D \right](s), \\
\mathcal{ST}[{}^{CF}D_0^{\wp} I_D(t)](s) &= \mathcal{ST}[\sigma_D^{\wp} E_D - (\gamma_D^{\wp} + \mu_D^{\wp}) I_D](s), \\
\mathcal{ST}[{}^{CF}D_0^{\wp} R_D(t)](s) &= \mathcal{ST}[\gamma_D^{\wp} I_D - (\eta_D^{\wp} + \mu_D^{\wp}) R_D](s).
\end{aligned} \tag{28}$$

Now by applying the Sumudu transform on the Caputo–Fabrizio Ebola model yields;

$$\begin{aligned}
\frac{\mho(\wp)}{1-\wp+\wp s}(\mathcal{ST}[S_H(t)](s) - S_H(0)) &= \mathcal{ST}\left[m_1^{\wp} - \frac{\beta_H^{\wp} S_H I_D}{1+\alpha_1 I_D} - \mu_H^{\wp} S_H + \eta_H^{\wp} R_H \right](s), \\
\frac{\mho(\wp)}{1-\wp+\wp s}(\mathcal{ST}[E_H(t)](s) - E_H(0)) &= \mathcal{ST}\left[\frac{\beta_H^{\wp} S_H I_D}{1+\alpha_1 I_D} - (\mu_H^{\wp} + \sigma_H^{\wp}) E_H \right](s), \\
\frac{\mho(\wp)}{1-\wp+\wp s}(\mathcal{ST}[I_H(t)](s) - I_H(0)) &= \mathcal{ST}[\sigma_H^{\wp} E_H - (\gamma_H^{\wp} + \delta_H^{\wp} + \mu_H^{\wp}) I_H](s), \\
\frac{\mho(\wp)}{1-\wp+\wp s}(\mathcal{ST}[R_H(t)](s) - R_H(0)) &= [\gamma_H^{\wp} I_H - (\eta_H^{\wp} + \mu_H^{\wp}) R_H](s),
\end{aligned} \tag{29}$$

$$\frac{\mho(\wp)}{1-\wp+\wp s}(\mathcal{ST}[S_D(t)](s)-S_D(0))=\mathcal{ST}\left[m_2^{\wp}-\frac{\beta_D^{\wp}S_DI_H}{1+\alpha_2I_H}-\mu_D^{\wp}S_D\right](s),$$
$$\frac{\mho(\wp)}{1-\wp+\wp s}(\mathcal{ST}[E_D(t)](s)-E_D(0))=\mathcal{ST}\left[\frac{\beta_D^{\wp}S_DI_H}{1+\alpha_2I_H}-(\sigma_D^{\wp}+\mu_D^{\wp})E_D\right](s),$$
$$\frac{\mho(\wp)}{1-\wp+\wp s}(\mathcal{ST}[I_D(t)](s)-I_D(0))=\mathcal{ST}[\sigma_D^{\wp}E_D-(\gamma_D^{\wp}+\mu_D^{\wp})I_D](s),$$
$$\frac{\mho(\wp)}{1-\wp+\wp s}(\mathcal{ST}[R_D(t)](s)-R_D(0))=\mathcal{ST}[\gamma_D^{\wp}I_D-(\eta_D^{\wp}+\mu_D^{\wp})R_D](s).$$

Eq. (29) can be reformulated as;

$$\begin{aligned}
\mathcal{ST}[S_H(t)](s)&=S_H(0)+\frac{1-\wp+\wp s}{\mho(\wp)}\mathcal{ST}\left[m_1^{\wp}-\frac{\beta_H^{\wp}S_HI_D}{1+\alpha_1I_D}-\mu_H^{\wp}S_H+\eta_H^{\wp}R_H\right](s),\\
\mathcal{ST}[E_H(t)](s)&=E_H(0)+\frac{1-\wp+\wp s}{\mho(\wp)}\mathcal{ST}\left[\frac{\beta_H^{\wp}S_HI_A}{1+\alpha_1I_D}-(\mu_H^{\wp}+\sigma_H^{\wp})E_H\right](s),\\
\mathcal{ST}[I_H(t)](s)&=I_H(0)+\frac{1-\wp+\wp s}{\mho(\wp)}\mathcal{ST}[\sigma_H^{\wp}E_H-(\gamma_H^{\wp}+\delta_H^{\wp}+\mu_H^{\wp})I_H](s),\\
\mathcal{ST}[R_H(t)](s)&=R_H(0)+\frac{1-\wp+\wp s}{\mho(\wp)}\mathcal{ST}[\gamma_H^{\wp}I_H-(\eta_H^{\wp}+\mu_H^{\wp})R_H](s),\\
\mathcal{ST}[S_D(t)](s)&=S_D(0)+\frac{\mho(\wp)}{1-\wp+\wp s}\mathcal{ST}\left[m_2^{\wp}-\frac{\beta_D^{\wp}S_DI_H}{1+\alpha_2I_H}-\mu_D^{\wp}S_D+\eta_D^{\wp}R_D\right](s),\\
\mathcal{ST}[E_D(t)](s)&=E_D(0)+\frac{1-\wp+\wp s}{\mho(\wp)}\mathcal{ST}\left[\frac{\beta_D^{\wp}S_DI_H}{1+\alpha_2I_H}-(\sigma_D^{\wp}+\mu_D^{\wp})E_D\right](s),\\
\mathcal{ST}[I_D(t)](s)&=I_D(0)+\frac{1-\wp+\wp s}{\mho(\wp)}\mathcal{ST}[\sigma_D^{\wp}E_D-(\gamma_D^{\wp}+\mu_D^{\wp})I_D](s),\\
\mathcal{ST}[R_D(t)](s)&=R_D(0)+\frac{1-\wp+\wp s}{\mho(\wp)}\mathcal{ST}[\gamma_D^{\wp}I_D-(\eta_D^{\wp}+\mu_D^{\wp})R_D](s).
\end{aligned}\tag{30}$$

Our focus is to derive iterative equations, and by taking the inverse of the Sumudu transform (28) gives us;

$$\begin{aligned}
S_{H\,i+1}(t)&=S_H(0)+\frac{1-\wp+\wp s}{\mho(\wp)}\mathcal{ST}^{-1}\left[m_1^{\wp}-\frac{\beta_H^{\wp}S_HI_A}{1+\alpha_1I_D}-\mu_H^{\wp}S_H+\eta^{\wp}R_H\right](s),\\
I_{H\,i+1}(t)&=E_H(0)+\frac{1-\wp+\wp s}{\mho(\wp)}\mathcal{ST}^{-1}\left[\frac{\beta_H^{\wp}S_HI_A}{1+\alpha_1I_D}-(\mu_H^{\wp}+\sigma_H^{\wp})E_H\right](s),\\
E_{H\,i+1}(t)&=I_H(0)+\frac{1-\wp+\wp s}{\mho(\wp)}\mathcal{ST}^{-1}[\sigma_H^{\wp}E_H-(\gamma_H^{\wp}+\delta_H^{\wp}+\mu_H^{\wp})I_H](s),\\
R_{H\,i+1}(t)&=R_H(0)+\frac{1-\wp+\wp s}{\mho(\wp)}\mathcal{ST}^{-1}[\gamma_H^{\wp}I_H-(\eta+\mu_H^{\wp})R_H](s),\\
S_{D\,i+1}(t)&=S_D(0)+\frac{\mho(\wp)}{1-\wp+\wp s}\mathcal{ST}^{-1}\left[m_2^{\wp}-\frac{\beta_D^{\wp}S_DI_H}{1+\alpha_2I_H}-\mu_D^{\wp}S_D+\eta_D^{\wp}R_D\right](s),\\
E_{D\,i+1}(t)&=E_D(0)+\frac{1-\wp+\wp s}{\mho(\wp)}\mathcal{ST}^{-1}\left[\frac{\beta_D^{\wp}S_DI_H}{1+\alpha_2I_H}-(\sigma_D^{\wp}+\mu_D^{\wp})E_D\right](s),\\
I_{D\,i+1}(t)&=I_D(0)+\frac{1-\wp+\wp s}{\mho(\wp)}\mathcal{ST}^{-1}[\sigma_D^{\wp}E_D-(\gamma_D^{\wp}+\mu_D^{\wp})I_D](s),\\
R_{D\,i+1}(t)&=R_D(0)+\frac{1-\wp+\wp s}{\mho(\wp)}\mathcal{ST}^{-1}[\gamma_D^{\wp}I_D-(\eta_D^{\wp}+\mu_D^{\wp})R_D](s).
\end{aligned}\tag{31}$$

The approximate solutions of the Caputo–Fabrizio Ebola model are given as

$$\lim_{i\longrightarrow\infty}S_{H\,i}(t)=S_H(t),\ \lim_{i\longrightarrow\infty}E_{H\,i}(t)=E_H(t),\ \lim_{i\longrightarrow\infty}I_{H\,i}(t)=I_H(t),\ \lim_{i\longrightarrow\infty}R_{H\,i}(t)=R_H(t),$$
$$\lim_{i\longrightarrow\infty}S_{D\,i}(t)=S_D(t),\ \lim_{i\longrightarrow\infty}E_{D\,i}(t)=S_E(t),\ \lim_{i\longrightarrow\infty}I_{D\,i}(t)=I_D(t),\ \lim_{i\longrightarrow\infty}R_{D\,i}(t)=R_D(t).$$

We then establish that the fractional Caputo–Fabrizio model is Sumudu transform stable by considering the theorem below. Before stating the theorem, we first define the following: $\Theta_1 = \frac{\beta_H^{\wp}}{1+\alpha_1 I_D}, \Theta_2 = \frac{\beta_D^{\wp}}{1+\alpha_2 I_H}$, we reformulate Eq. (3) as;

$$\begin{aligned}
{}^{CF}D_0^{\wp} S_H(t) &= m_1^{\wp} - \Theta_1 S_H I_D - \mu_H^{\wp} S_H + \eta_H^{\wp} R_H,\\
{}^{CF}D_0^{\wp} E_H(t) &= \Theta_1 S_H I_D - (\mu_H^{\wp} + \sigma_H^{\wp}) E_H,\\
{}^{CF}D_0^{\wp} I_H(t) &= \sigma_H^{\wp} E_H - (\gamma_H^{\wp} + \delta_H^{\wp} + \mu_H^{\wp}) I_H,\\
{}^{CF}D_0^{\wp} R_H(t) &= \gamma_H^{\wp} I_H - (\eta_H^{\wp} + \mu_H^{\wp}) R_H,\\
{}^{CF}D_0^{\wp} S_D(t) &= m_2^{\wp} - \Theta_2 S_D I_H - \mu_D^{\wp} S_D + \eta_D^{\wp} R_D,\\
{}^{CF}D_0^{\wp} E_D(t) &= \Theta_2 S_D I_H - (\sigma_D^{\wp} + \mu_D^{\wp}) E_D,\\
{}^{CF}D_0^{\wp} I_D(t) &= \sigma_D^{\wp} E_D - (\gamma_D^{\wp} + \mu_D^{\wp}) I_D,\\
{}^{CF}D_0^{\wp} R_D(t) &= \gamma_D^{\wp} I_D - (\eta_D^{\wp} + \mu_D^{\wp}) R_D.
\end{aligned} \tag{32}$$

Theorem 5. *Let us presume that Π represents a self map which is given below:*

$$\begin{aligned}
\Pi(S_{H\,i}(t)) = S_{H\,i+1}(t) &= S_H(0) + \frac{1-\wp+\wp s}{\mho(\wp)} \mathcal{ST}^{-1}\left[m_1^{\wp} - \frac{\beta_H^{\wp} S_H I_D}{1+\alpha_1 I_D} - \mu_H^{\wp} S_H + \eta_H^{\wp} R_H\right](s),\\
\Pi(I_{H\,i}(t)) = I_{H\,i+1}(t) &= E_H(0) + \frac{1-\wp+\wp s}{\mho(\wp)} \mathcal{ST}^{-1}\left[\frac{\beta_H^{\wp} S_H I_D}{1+\alpha_1 I_D} - (\mu_H^{\wp} + \sigma_H^{\wp}) E_H\right](s),\\
\Pi(E_{H\,i}(t)) = E_{H\,i+1}(t) &= \mathcal{I}_H(0) + \frac{1-\wp+\wp s}{\mho(\wp)} \mathcal{ST}^{-1}[\sigma_H^{\wp} E_H - (\gamma_H^{\wp} + \delta_H^{\wp} + \mu_H^{\wp}) I_H](s),\\
\Pi(R_{H\,i}(t)) = R_{H\,i+1}(t) &= R_H(0) + \frac{1-\wp+\wp s}{\mho(\wp)} \mathcal{ST}^{-1}[\gamma_H^{\wp} I_H - (\eta_H + \mu_H^{\wp}) R_H](s),\\
\Pi(S_{D\,i}(t)) = S_{D\,i+1}(t) &= S_D(0) + \frac{\mho(\wp)}{1-\wp+\wp s} \mathcal{ST}^{-1}\left[m_2^{\wp} - \frac{\beta_D^{\wp} S_D I_H}{1+\alpha_2 I_H} - \mu_D^{\wp} S_D + \eta_D^{\wp} R_D\right](s),\\
\Pi(E_{D\,i}(t)) = E_{D\,i+1}(t) &= E_D(0) + \frac{1-\wp+\wp s}{\mho(\wp)} \mathcal{ST}^{-1}\left[\frac{\beta_D^{\wp} S_D I_H}{1+\alpha_2 I_H} - (\sigma_D^{\wp} + \mu_D^{\wp}) E_D\right](s),\\
\Pi(I_{D\,i}(t)) = I_{D\,i+1}(t) &= I_D(0) + \frac{1-\wp+\wp s}{\mho(\wp)} \mathcal{ST}^{-1}[\sigma_D^{\wp} E_D - (\gamma_D^{\wp} + \mu_D^{\wp}) I_D](s),\\
\Pi(R_{D\,i}(t)) = R_{D\,i+1}(t) &= R_D(0) + \frac{1-\wp+\wp s}{\mho(\wp)} \mathcal{ST}^{-1}[\gamma_D^{\wp} I_D - (\eta_D^{\wp} + \mu_D^{\wp}) R_D](s),
\end{aligned} \tag{33}$$

then we say that the recursive fractional Caputo–Fabrizio model (3) is $\Pi-$ stable in $\mathcal{B}^1(a,b)$ whenever we have

$$\begin{aligned}
&1 - \Theta_1 M_1^* \Psi_1 - \Theta_2 M_2^* \Psi_2 - \mu_H^{\wp} \Psi_3^* + \eta_H^{\wp} \Psi_4^*,\\
&1 + \Theta_3 M_1^* \Psi_5 + \Theta_4 M_2^* \Psi_6 - (\mu_H^{\wp} + \sigma_H^{\wp}) \Psi_7,\\
&1 + \sigma_H^{\wp} \Psi_8 - (\gamma_H^{\wp} + \delta_H^{\wp} + \mu_H^{\wp}) \Psi_9,\\
&1 + \gamma_H \Psi_{10} - (\eta_H + \mu_H^{\wp}) \Psi_{11},\\
&1 - \Theta_5 M_3^* \Psi_{12} - \Theta_6 M_4^* \Psi_{13} - \mu_D^{\wp} \Psi_{14} + \eta_D^{\wp} \Psi_{15},\\
&1 + \Theta_7 M_3^* \Psi_{16} - \Theta_8 M_4^* \Psi_{17} - (\sigma_D^{\wp} + \mu_D^{\wp}) \Psi_{18},\\
&1 + \sigma_D^{\wp} \Psi_{19} - (\gamma_D^{\wp} + \mu_D^{\wp}) \Psi_{20},\\
&1 + \gamma_D^{\wp} \Psi_{21} - (\eta_D^{\wp} + \mu_D^{\wp}) \Psi_{22},
\end{aligned} \tag{34}$$

given that Ψ_i for $i = 1, 2, 3, \ldots, 22$ are some introduced functions.

Proof. In the preliminary phases of this proof, we prove that the transform $\Pi-$ possesses a fixed starting point. For any natural numbers n and m, it is true that;

$$\begin{aligned}
\|\Pi(S_{H\,n}(t)) - \Pi(S_{H\,m}(t))\| &= \|(S_{H\,n+1}(t)) - (S_{H\,m+1}(t))\|,\\
&= \|S_{H\,n}(t) + \mathcal{ST}^{-1}\left[\frac{1-\wp+\wp s}{\mho(\wp)} \mathcal{ST}[m_1 - \Theta_1 S_H I_D - \mu_H S_H + \eta_H R_H](s)\right] - S_{H\,m}(t)\\
&- \mathcal{ST}\left[\frac{1-\wp+\wp s}{\mho(\wp)} \mathcal{ST}[m_1 - \Theta_1 S_H I_D - \mu_H S_H + \eta_H R_H](s)\right]\|,\\
&\le \|(S_{Hn+1}(t)) - (S_{Hm+1}(t))\| + \|\mathcal{ST}^{-1}[\frac{1-\wp+\wp s}{\mho(\wp)} - \Theta_1(S_{H\,n} I_{D\,n} - S_{H\,m} I_{D\,m})\\
&- \mu_H^{\wp}(S_{H\,n} - S_{H\,m}) + \eta^{\wp}(R_{Hn} - R_{Hm})](s),
\end{aligned}$$

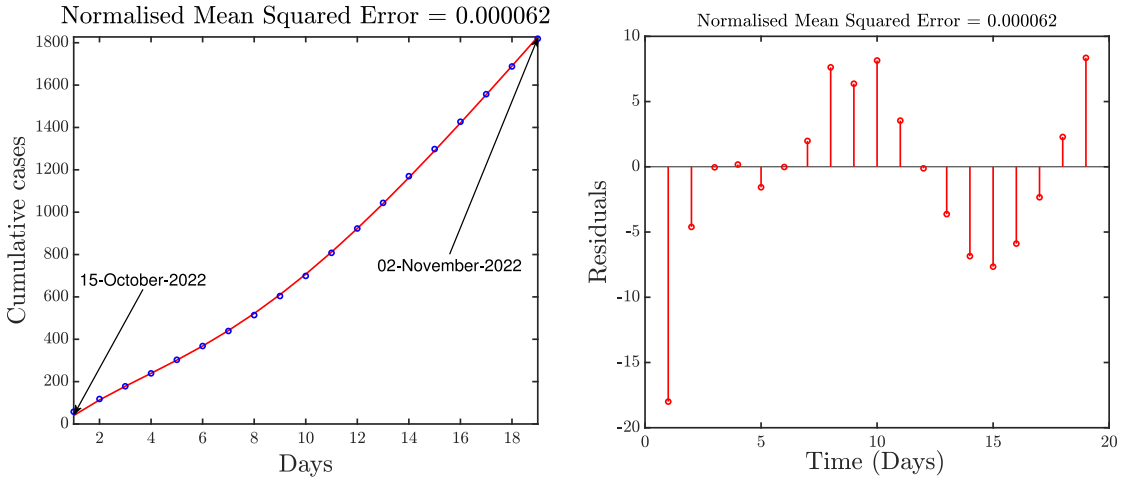

(a) Model fit (b) Residual plot

Fig. 1. Propose Ebola human & dog model verse cumulative Ebola human cases and residuals.

$$\leq \|(S_{H\,n+1}(t)) - (S_{H\,m+1}(t))\| + \|\mathcal{ST}^{-1}[\frac{1-\wp+\wp s}{\mho(\wp)} - \|\Theta_1 S_{Hn}(I_{Dn} - I_{Dm})\|$$
$$- \|\mu_H^{\wp}(S_{Hn} - S_{Hm})\| + \|\eta^{\wp}(R_{Hn} - R_{Hm})](s)\|. \tag{35}$$

Similar results are determined for the other compartmental states, and since all of the eight solutions have similar roles, we consider;

$$\|S_{Hn}(t) - S_{Hm}(t)\| \cong \|E_{Hn}(t) - E_{Hm}(t)\| \cong \|I_{Hn}(t) - I_{Hm}(t)\| \cong \|R_{Hn}(t) - R_{Hm}(t)\|$$
$$\cong \|S_{Dn}(t) - S_{Dm}(t)\| \cong \|E_{Dn}(t) - E_{Dm}(t)\| \cong \|I_{Dn}(t) - I_{Dm}(t)\| \cong \|R_{Dn}(t) - R_{Dm}(t)\|. \tag{36}$$

From Eqs. (35) and (36) we have;

$$\|\Pi(S_{H\,n}(t)) - \Pi(S_{H\,m}(t))\| = \|(S_{H\,n+1}(t)) - (S_{H\,m+1}(t))\|,$$
$$\leq \|(S_{H\,n+1}(t)) - (S_{H\,m+1}(t))\| + \|\mathcal{ST}^{-1}[\frac{1-\wp+\wp s}{\mho(\wp)} m_1^{\wp} - \|\Theta_1 S_{Hn}(S_{Hn} - S_{Hm})\|,$$
$$- \|\mu_H^{\wp}(S_{H\,n} - S_{H\,m})\| + \|\eta^{\wp}(S_{Hn} - S_{Hm})](s)\|. \tag{37}$$

It is therefore observed that $S_{Hn}, E_{Hn}, I_{Hn}, R_{Hn}, S_{Dn}, E_{Dn}, I_{Dn}$ and R_{Dn} are convergent sequences and thus bounded. Therefore, there exist the boundedness constants $M_1^*, M_2^*, M_3^*, M_4^*, M_5^*, M_6^*, M_7^*$, and M_8^* so that for every t and $m, n \in \mathbb{N}$, yields;

$$\|S_{Hn}\| \leq M_1^*, \quad \|E_{Hn}\| \leq M_2^*, \quad \|I_{Hn}\| \leq M_3^*, \quad \|R_{Hn}\| \leq M_4^*,$$

$$\|S_{Dn}\| \leq M_5^*, \quad \|E_{Dn}\| \leq M_6^*, \quad \|I_{Dn}\| \leq M_7^*, \quad \|R_{Dn}\| \leq M_8^*.$$

We, therefore, have:

$$\|\Pi(S_{H\,n}(t)) - \Pi(S_{H\,m}(t))\| = \|(S_{H\,n+1}(t)) - (S_{H\,m+1}(t))\|,$$
$$\leq \|(S_{H\,n+1}(t)) - (S_{H\,m+1}(t))\| + \|\mathcal{ST}^{-1}[\frac{1-\wp+\wp s}{\mho(\wp)} \mathcal{ST}[-\Theta_1 M_1^* \|(S_{Hn} - S_{Hm})\|$$
$$- \mu_H^{\wp}\|(S_{Hn} - S_{Hm})\| + \eta^{\wp}\|(S_{Hn} - S_{Hm})\|](s)],$$
$$= \left(1 - \Theta_1 M_1^* \Psi_1 - \Theta_2 M_2^* \Psi_2 - \mu_H^{\wp}\Psi_3^* + \eta_H^{\wp}\Psi_4^*\right) \|(S_{Hn} - S_{Hm})\|, \tag{38}$$

where $\Psi_i, i = 1, 2, \ldots, 29$ indicates functions derived from the inverse transform $\mathcal{ST}^{-1}\left[\frac{1-\wp+\wp s}{\mho(\wp)}\right]$. It follows that the other state variables also yield similar results, as given below:

$$\|\Pi(E_{Hn}(t)) - \Pi(S_{Hm}(t))\| = \left(1 + \Theta_3 M_1^* \Psi_5 + \Theta_4 M_2^* \Psi_6 - (\mu_H^{\wp} + \sigma_H^{\wp})\Psi_7\right) \|(E_{Hn} - E_{Hm})\|,$$
$$\|\Pi(I_{Hn}(t)) - \Pi(I_{Hm}(t))\| = \left(1 + \sigma_H^{\wp}\Psi_8 - (\gamma_H^{\wp} + \delta_H^{\wp} + \mu_H^{\wp})\Psi_9\right) \|(I_{Hn} - I_{Hm})\|,$$
$$\|\Pi(R_{Hn}(t)) - \Pi(R_{Hm}(t))\| = \left(1 + \gamma_H \Psi_{10} - (\eta_H + \mu_H^{\wp})\Psi_{11}\right) \|(R_{Hn} - R_{Hm})\|, \tag{39}$$
$$\|\Pi(S_{Dn}(t)) - \Pi(S_{Dm}(t))\| = \left(1 - \Theta_5 M_3^* \Psi_{12} - \Theta_6 M_4^* \Psi_{13} - \mu_D^{\wp}\Psi_{14} + \eta_D^{\wp}\Psi_{15}\right) \|(S_{Dn} - S_{Dm})\|,$$
$$\|\Pi(E_{Dn}(t)) - \Pi(E_{Dm}(t))\| = \left(1 + \Theta_7 M_3^* \Psi_{16} - \Theta_8 M_4^* \Psi_{117} - (\sigma_D^{\wp} + \mu_D^{\wp})\Psi_{18}\right) \|(E_{Dn} - E_{Dm})\|,$$

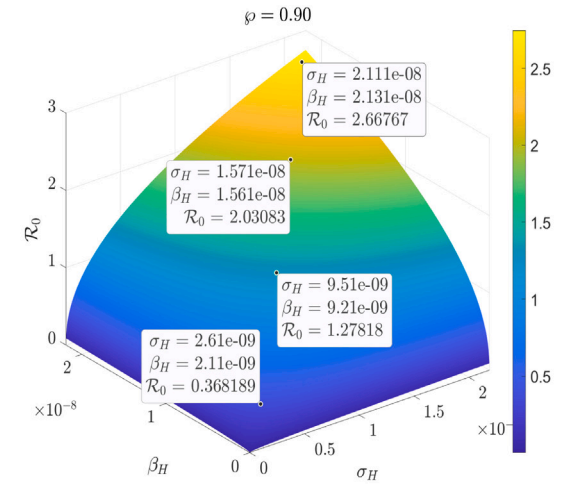

(a) Effect of β_H and σ_H on $\mathcal{R}_0$

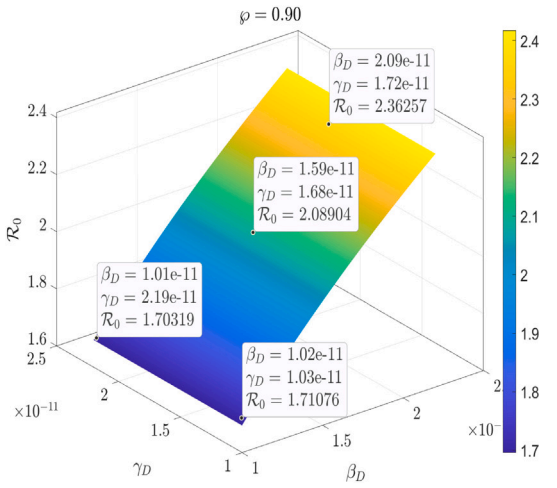

(b) Effect of γ_D and β_D on $\mathcal{R}_0$

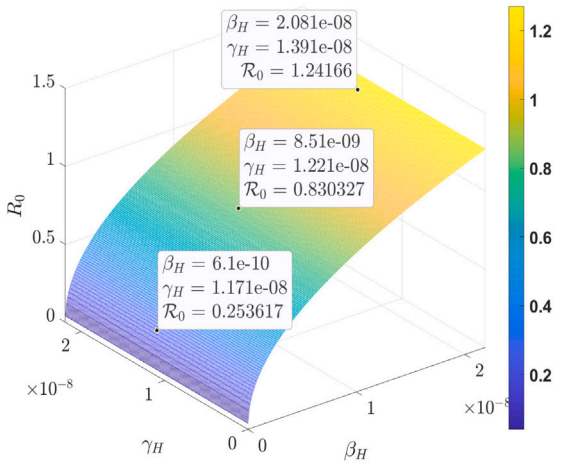

(c) Effect of γ_H and β_H on $\mathcal{R}_0$

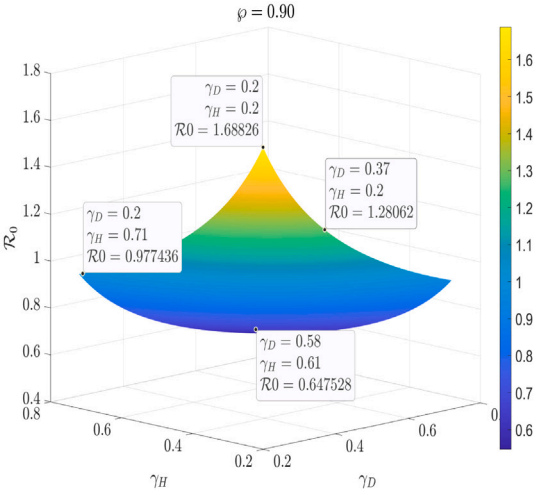

(d) Effect of γ_H and γ_D on $\mathcal{R}_0$

Fig. 2. Effects of $\beta_H, \beta_D, \gamma_H, \gamma_D$ and σ_H on $\mathcal{R}_0$.

$$\|\Pi(I_{Dn}(t)) - \Pi(I_{Dm}(t))\| = \left(1 + \sigma_D^{\wp}\Psi_{19} - (\gamma_D^{\wp} + \mu_D^{\wp})\Psi_{20}\right) \|(I_{Dn} - I_{Dm})\|,$$
$$\|\Pi(I_{Dn}(t)) - \Pi(I_{Dm}(t))\| = \left(1 + \gamma_D^{\wp}\Psi_{21} - (\eta_D^{\wp} + \mu_D^{\wp})\Psi_{22}\right) \|(I_{Dn} - I_{Dm})\|,$$

It is therefore observed that, given the hypothesis (34), the self-map Ψ has a fixed point since it is a contraction. In consequence, we say that the self-map Ψ suffices the assumptions of the theorem and

$$\begin{aligned}
&1 - \Theta_1 M_1^* \Psi_1 - \Theta_2 M_2^* \Psi_2 - \mu_H^{\wp}\Psi_3^* + \eta_H^{\wp}\Psi_4^*,\\
&1 + \Theta_3 M_1^* \Psi_5 + \Theta_4 M_2^* \Psi_6 - (\mu_H^{\wp} + \sigma_H^{\wp})\Psi_7,\\
&1 + \sigma_H^{\wp}\Psi_8 - (\gamma_H^{\wp} + \delta_H^{\wp} + \mu_H^{\wp})\Psi_9,\\
&1 + \gamma_H \Psi_{10} - (\eta_H^{\wp} + \mu_H^{\wp})\Psi_{11},\\
&1 - \Theta_5 M_3^* \Psi_{12} - \Theta_6 M_4^* \Psi_{13} - \mu_D^{\wp}\Psi_{14} + \eta_D^{\wp}\Psi_{15},\\
&1 + \Theta_7 M_3^* \Psi_{16} - \Theta_8 M_4^* \Psi_{17} - (\sigma_D^{\wp} + \mu_D^{\wp})\Psi_{18},\\
&1 + \sigma_D^{\wp}\Psi_{19} - (\gamma_D^{\wp} + \mu_D^{\wp})\Psi_{20},\\
&1 + \gamma_D^{\wp}\Psi_{21} - (\eta_D^{\wp} + \mu_D^{\wp})\Psi_{22}.
\end{aligned} \tag{40}$$

Therefore, it is observed that Ψ is a Picard $\Psi-$ stable. Hence proved.

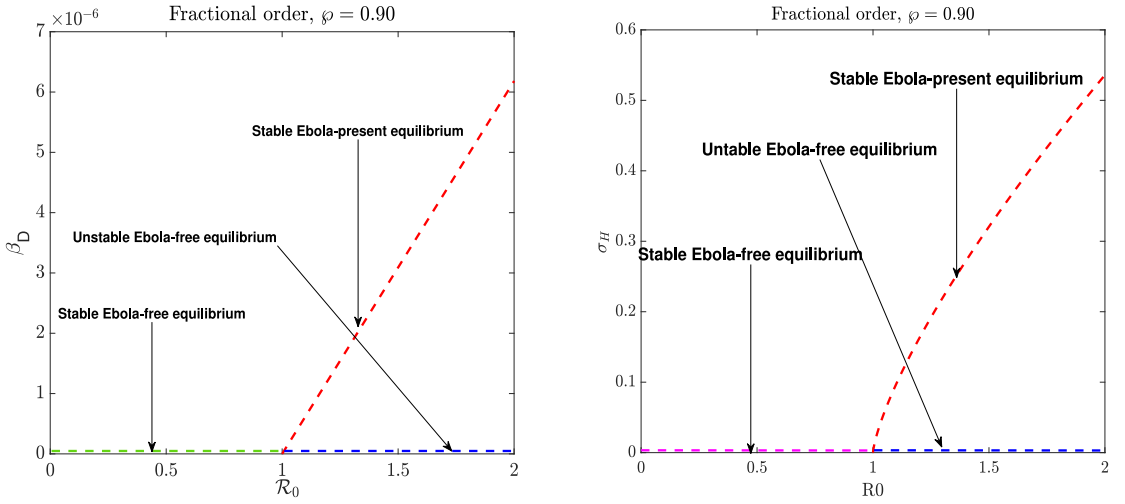

(a) Forward bifurcation with varying β_D

(b) Forward bifurcation with varying σ_H

Fig. 3. Forward bifurcation plots.

Numerical technique for the Ebola model

Here, we present a numerical scheme for the fractional operator used in studying Ebola transmission. We thus employ a two-step Lagrange interpolation to derive a numerical scheme for the Caputo–Fabrizio derivative. Given the Cauchy problem

$$^{CF}D_t^{\varrho}\mathcal{B}(t) = \mathbb{N}(t, \mathcal{B}(t)), \tag{41}$$

and the Caputo–Fabrizio derivative is therefore given as

$$\mathcal{B}(t) = \mathcal{B}_0(t) + \frac{(1-\varrho)}{\mathfrak{O}(\varrho)}\mathbb{N}(t, \mathcal{B}(t)) + \frac{\varrho}{\mathfrak{O}(\varrho)}\int_0^t \mathbb{N}(t, \mathcal{B}(\tau))d\tau. \tag{42}$$

We then use a recursive approach to reformulate Eq. (42) by considering the equation at the point $t_\lambda = (\lambda)h$ and also $t_{\lambda+1} = (\lambda+1)h$, where h is defined as the step size or time step and $\lambda = 1, 2, 3, \ldots$. This yields;

$$\mathcal{B}(t_\lambda) = \mathcal{B}(0) + \frac{(1-\varrho)}{\mathfrak{O}(\varrho)}\mathbb{N}(t_{\lambda-1}, \mathcal{B}(t\lambda - 1)) + \frac{\varrho}{\mathfrak{O}(\varrho)}\int_{t_\lambda}^{t_{\lambda+1}} \mathbb{N}(t, \mathcal{B}(\tau))d\tau, \tag{43}$$

and

$$\mathcal{B}(t_{\lambda+1}) = \mathcal{B}(0) + \frac{(1-\varrho)}{\mathfrak{O}(\varrho)}\mathbb{N}(t_\lambda, \mathcal{B}(t\lambda)) + \frac{\varrho}{\mathfrak{O}(\varrho)}\int_{t_\lambda}^{t_{\lambda+1}} \mathbb{N}(t, \mathcal{B}(\tau))d\tau. \tag{44}$$

Now, by subtracting Eq. (43) from Eq. (44), we have:

$$\mathcal{B}(t_{\lambda+1}) = \mathcal{B}(0) + \frac{(1-\varrho)}{\mathfrak{O}(\varrho)}[\mathbb{N}(t_\lambda, \mathcal{B}(t_\lambda)) - \mathbb{N}(t_{\lambda-1}, \mathcal{B}(t_{\lambda-1}))] + \frac{\varrho}{\mathfrak{O}(\varrho)}\int_{t_\lambda}^{t_{\lambda+1}} \mathbb{N}(t, \mathcal{B}(\tau))d\tau. \tag{45}$$

We then apply the Lagrange two-step polynomial to Eq. (45); this suffices.

$$\begin{aligned}\mathcal{B}(t_{\lambda+1}) - \mathcal{B}(t_\lambda) = {} & \frac{(1-\varrho)}{\mathfrak{O}(\varrho)}[\mathbb{N}(t_\lambda, \mathcal{B}(t_\lambda)) - \mathbb{N}(t_{\lambda-1}, \mathcal{B}(t_{\lambda-1}))] + \frac{\varrho}{\mathfrak{O}(\varrho)} \\ & \times \int_{t_\lambda}^{t_{\lambda+1}} \left[\frac{\mathbb{N}(t_\lambda, \mathcal{B}(t_\lambda))}{h}(\tau - t_{\lambda-1}) - \frac{\mathbb{N}(t_{\lambda-1}, \mathcal{B}(t_{\lambda-1}))}{h}(\tau - t_\lambda)\right] d\tau.\end{aligned} \tag{46}$$

Which further yields

$$\begin{aligned}\mathcal{B}(t_{\lambda+1}) - \mathcal{B}(t_\lambda) = {} & \frac{(1-\varrho)}{\mathfrak{O}(\varrho)}[\mathbb{N}(t_\lambda, \mathcal{B}(t_\lambda)) - \mathbb{N}(t_{\lambda-1}, \mathcal{B}(t_{\lambda-1}))] + \frac{\varrho}{\mathfrak{O}(\varrho)} \\ & \times \left[\frac{\mathbb{N}(t_\lambda, \mathcal{B}(t_\lambda))}{h}\int_{t_\lambda}^{t_{\lambda+1}}(\tau - t_{\lambda-1})d\tau - \frac{\mathbb{N}(t_{\lambda-1}, \mathcal{B}(t_{\lambda-1}))}{h}\int_{t_\lambda}^{t_{\lambda+1}}(\tau - t_\lambda)d\tau\right].\end{aligned} \tag{47}$$

We simplify Eq. (47) further by evaluating the integrals in there, and this leads to:

$$\mathcal{B}_{\lambda+1} = \mathcal{B}_\lambda + \left[\frac{(1-\varrho)}{\mathfrak{O}(\varrho)} + \frac{3h\varrho}{2\mathfrak{O}(\varrho)}\right]\mathbb{N}(t_\lambda, \mathcal{B}(t_\lambda)) - \left[\frac{(1-\varrho)}{\mathfrak{O}(\varrho)} + \frac{h\varrho}{2\mathfrak{O}(\varrho)}\right]\mathbb{N}(t_{\lambda-1}, \mathcal{B}_{\lambda-1}), \tag{48}$$

where

$$\int_{t_\lambda}^{t_{\lambda+1}} (\tau - t_\lambda) d\tau = \frac{1}{2}h^2, \quad \int_{t_\lambda}^{t_{\lambda+1}} (\tau - t_{\lambda-1}) d\tau = \frac{2}{2}h^2, \tag{49}$$

and Eq. (49) is the Caputo–Fabrizio numerical scheme. We then apply this numerical scheme to the Ebola model, and we have;

$$\begin{aligned}
S_{H\lambda+1} &= S_{H\lambda} + \left[\frac{(1-\varrho)}{\mho(\varrho)} + \frac{3h\varrho}{2\mho(\varrho)}\right]\mathbb{N}(t_\lambda, S_{H\lambda}) - \left[\frac{(1-\varrho)}{\mho(\varrho)} + \frac{h\varrho}{2\mho(\varrho)}\right]\mathbb{N}(t_{\lambda-1}, S_{H\lambda-1}),\\
E_{H\lambda+1} &= E_{H\lambda} + \left[\frac{(1-\varrho)}{\mho(\varrho)} + \frac{3h\varrho}{2\mho(\varrho)}\right]\mathbb{N}(t_\lambda, E_{H\lambda}) - \left[\frac{(1-\varrho)}{\mho(\varrho)} + \frac{h\varrho}{2\mho(\varrho)}\right]\mathbb{N}(t_{\lambda-1}, E_{H\lambda-1}),\\
I_{H\lambda+1} &= I_{H\lambda} + \left[\frac{(1-\varrho)}{\mho(\varrho)} + \frac{3h\varrho}{2\mho(\varrho)}\right]\mathbb{N}(t_\lambda, I_{H\lambda}) - \left[\frac{(1-\varrho)}{\mho(\varrho)} + \frac{h\varrho}{2\mho(\varrho)}\right]\mathbb{N}(t_{\lambda-1}, I_{H\lambda-1}),\\
R_{H\lambda+1} &= R_{H\lambda} + \left[\frac{(1-\varrho)}{\mho(\varrho)} + \frac{3h\varrho}{2\mho(\varrho)}\right]\mathbb{N}(t_\lambda, R_{H\lambda}) - \left[\frac{(1-\varrho)}{\mho(\varrho)} + \frac{h\varrho}{2\mho(\varrho)}\right]\mathbb{N}(t_{\lambda-1}, R_{H\lambda-1}),\\
S_{D\lambda+1} &= S_{D\lambda} + \left[\frac{(1-\varrho)}{\mho(\varrho)} + \frac{3h\varrho}{2\mho(\varrho)}\right]\mathbb{N}(t_\lambda, S_{D\lambda}) - \left[\frac{(1-\varrho)}{\mho(\varrho)} + \frac{h\varrho}{2\mho(\varrho)}\right]\mathbb{N}(t_{\lambda-1}, S_{D\lambda-1}),\\
E_{D\lambda+1} &= E_{D\lambda} + \left[\frac{(1-\varrho)}{\mho(\varrho)} + \frac{3h\varrho}{2\mho(\varrho)}\right]\mathbb{N}(t_\lambda, E_{D\lambda}) - \left[\frac{(1-\varrho)}{\mho(\varrho)} + \frac{h\varrho}{2\mho(\varrho)}\right]\mathbb{N}(t_{\lambda-1}, E_{D\lambda-1}),\\
I_{D\lambda+1} &= I_{D\lambda} + \left[\frac{(1-\varrho)}{\mho(\varrho)} + \frac{3h\varrho}{2\mho(\varrho)}\right]\mathbb{N}(t_\lambda, I_{D\lambda}) - \left[\frac{(1-\varrho)}{\mho(\varrho)} + \frac{h\varrho}{2\mho(\varrho)}\right]\mathbb{N}(t_{\lambda-1}, I_{D\lambda-1}),\\
R_{D\lambda+1} &= R_{D\lambda} + \left[\frac{(1-\varrho)}{\mho(\varrho)} + \frac{3h\varrho}{2\mho(\varrho)}\right]\mathbb{N}(t_\lambda, R_{D\lambda}) - \left[\frac{(1-\varrho)}{\mho(\varrho)} + \frac{h\varrho}{2\mho(\varrho)}\right]\mathbb{N}(t_{\lambda-1}, R_{D\lambda-1}).
\end{aligned} \tag{50}$$

Parameter estimation and numerical simulations

In this section, we carried out parameter estimation, numerical sensitivity analysis, three-dimensional plots, forward bifurcation plots, and fractional two-dimensional numerical simulations. Furthermore, we varied the transmission rate and other parameters to check its sensitiveness to the proposed model.

Parameter estimation

Parameter estimation is crucial in epidemiological models. This method is a highly effective way to produce the most practical curve based on real data while also uncovering the parameters that are more accurate to their actual values [58–61]. The following text clarifies this approach's fundamental premise: The least-squares method can determine the model's parameters. Therefore, the data collected from the epidemic is used to adjust the solution of the model precisely. We employ the least squares method to analyse the model specified in Eq. (2). The procedure entails choosing initial approximations and pre-estimated parameters $\hat{k}$ for the model that offers the optimal fit or encompasses all the data points [62,63] through the minimisation of the sum of squared deviations between the observed data and the model solution $M(\mathbf{h}, \hat{k})$, such that

$$\mathcal{M}(\hat{k}) = \sum_{\mathbf{h}=1}^{l} (\hat{k}_{\mathbf{h}} - M(\mathbf{h}, \hat{k}))^2. \tag{51}$$

The data for the model fitting is taken from the Ugandan Ebola cases from October 15, 2022, and November 2, 2022; see Table 2. The data set is obtained from GitHub, as indicated in the works [64,65] that the data were obtained from the ECDC surveillance and Ministry of Health Uganda bulletins in collaboration with the World Health Organization's Regional Office for Africa (WHO AFRO). The worldometer indicated the total population of Ugandans in 2022 to be 47,249,585 [66]. Therefore, we considered the Ugandan human population $N_H^0 = 47249585$. According to the data in Table 2, the initial reported case of Ebola in Uganda was 58; thus, to get a reasonable fit of the proposed model to the actual data, we divided the 58 cases on October 15, 2022, into three categories. Thus, we assumed that the initial exposed humans would be $E_H^0 = 10$, recovered humans would be $R_H^0 = 18$, and symptomatic humans would be $I_H^0 = 30$, and hence the number of initial susceptible humans is calculated as $S_H^0 := N_H^0 - (E_H^0 + I_H^0 + R_H^0) = 47249527$. According to the World Health Organisation, the incubation period, or the interval between infection and the onset of symptoms, typically ranges from 2 to 21 days [67]. For the fitting, the initial guess for the rate at which people exposed to Ebola spread to the infectious class σ_H is $\sigma_H = \frac{1}{11.5}$. The life expectancy of Ugandans was 64.06 years [68]. Hence, the natural death rate of humans is estimated as $\mu_H = \frac{1}{(64.06\times365)}$. Therefore, the recruitment rate of humans is calculated as $m_1 = \mu_H \times N_H^0$. From the regional and continental estimates, the human-to-dog ratio in Uganda is 25 persons per dog [69]. Therefore, we considered the total number of dogs in Uganda to be $N_D^0 = \frac{47249585}{25}$. The assumed initial conditions for the exposed dogs are taken to be $E_D^0 = 100$, recovered dogs are taken to be $R_D^0 = 15$, and symptomatic dogs are taken to be $I_D^0 = 20$. Hence, the number of initial susceptible dog populations is calculated as $S_D^0 := N_D^0 - (E_D^0 + I_D^0 + R_D^0) = 1889848.4$. The life expectancy of dogs in Uganda is 10–14 years [70]. We assumed an

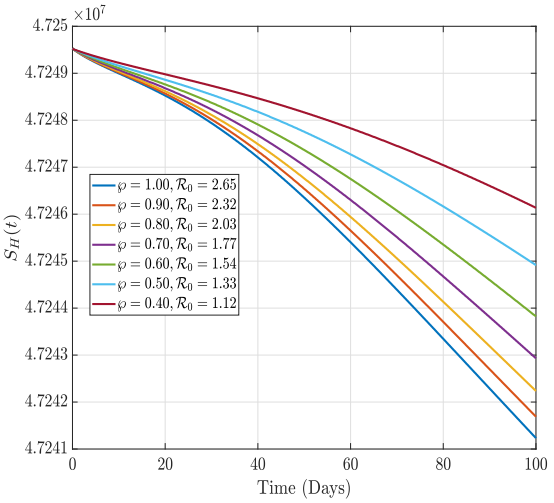

(a) The transmission pattern of $S_H(t)$ for several φ points.

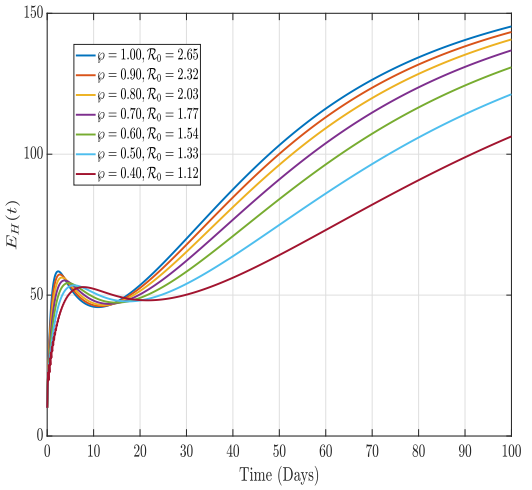

(b) The transmission pattern of $E_H(t)$ for several φ points.

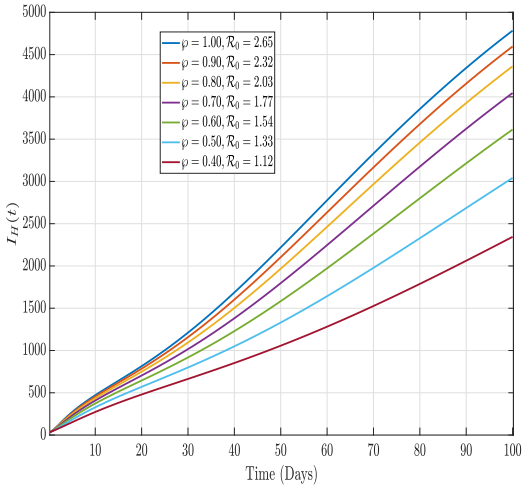

(c) The transmission pattern of $I_H(t)$ for several φ points.

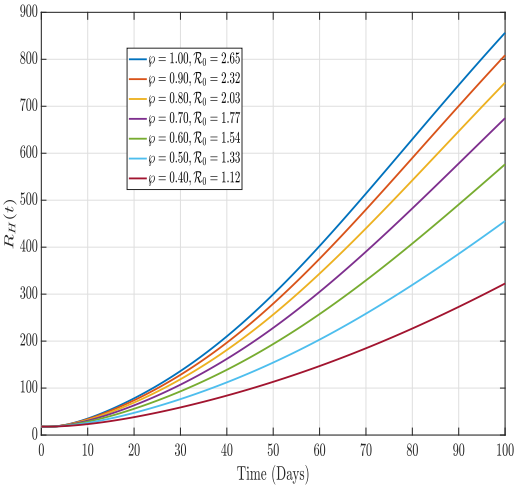

(d) The transmission pattern of $R_H(t)$ for several φ points.

Fig. 4. The transmission pattern of $S_H(t), E_H(t), I_H(t)$ and $R_H(t)$ for several φ points.

Table 2
Ebola human cases, from October 15, 2022, and November 2, 2022.

Dates	Daily cumulative	Cumulative cases	Dates	Daily cumulative	Cumulative cases
15/10/2022	58	58	24/10/2022	95	699
16/10/2022	60	118	25/10/2022	109	808
17/10/2022	60	178	26/10/2022	115	923
18/10/2022	61	239	27/10/2022	121	1044
19/10/2022	64	303	28/10/2022	126	1170
20/10/2022	65	368	29/10/2022	128	1298
21/10/2022	71	439	30/10/2022	129	1427
22/10/2022	75	514	31/10/2022	130	1557
23/10/2022	90	604	01/11/2022	131	1688
			02/11/2022	131	1819

initial guess of the natural death rate of dogs as $\mu_D = \frac{1}{12\times365}$. The recruitment rate of dogs is estimated as $m_2 = \mu_D \times N_D^0$. The model fit to the total data in Table 2 is shown in Fig. 1(a), and the residuals are shown in Fig. 1(b). This was done using the information above and some guesses about the parameters. From the model calibration in Fig. 1, the model parameters are presented in Table 3.

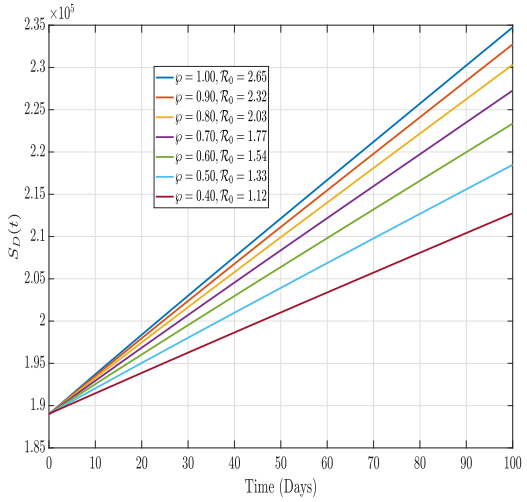

(a) The transmission pattern of $S_D(t)$ for several $\wp$ points.

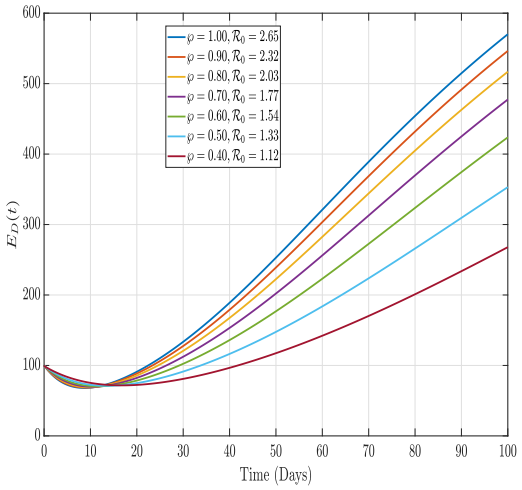

(b) The transmission pattern of $E_D(t)$ for several $\wp$ points.

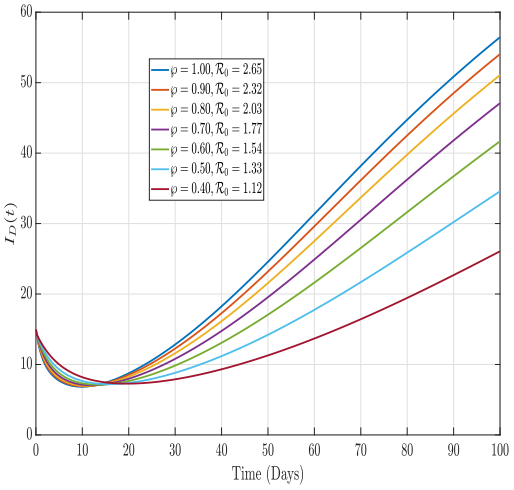

(c) The transmission pattern of $I_D(t)$ for several $\wp$ points.

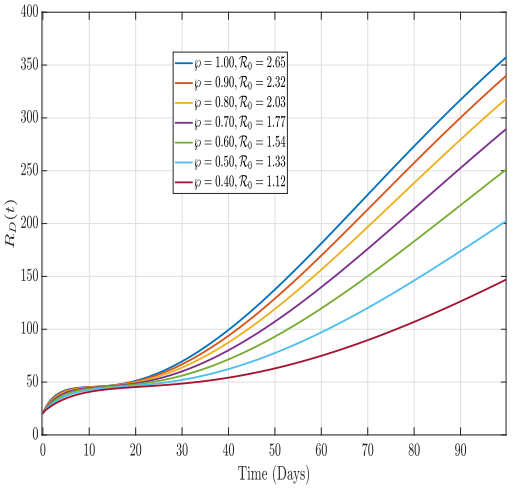

(d) The transmission pattern of $R_D(t)$ for several $\wp$ points.

Fig. 5. The transmission pattern of $S_D(t), E_D(t), I_D(t)$ and $R_D(t)$ for several $\wp$ points.

Table 3
The Ebola model parameter values.

Model parameter	Values/day	Source	Model parameter	Values/day	Source
m_1	2020	Estimated	μ_D	0.000230	Fitted
m_2	515	Fitted	δ_H	0.01078	Fitted
β_H	1.65×10^{-8}	Fitted	γ_H	0.010793	Fitted
β_D	8.0×10^{-8}	Fitted	γ_D	0.912204	Fitted
α_1	0.040698	Fitted	η_H	0.047585	Fitted
α_2	0.000117	Fitted	η_D	0.132617	Fitted
μ_H	$\frac{1}{(64.06\times365)}$	Estimated	σ_H	0.0998579	Fitted
			σ_D	0.091280	Fitted

Sensitivity analysis of the Ebola reproduction number

In this part, a sensitivity analysis is performed to identify the parameters which exert the most significant influence on the variable $\mathcal{R}_0$. Utilising sensitivity is important in identifying key parameters when formulating intervention strategies [71,72]. Here,

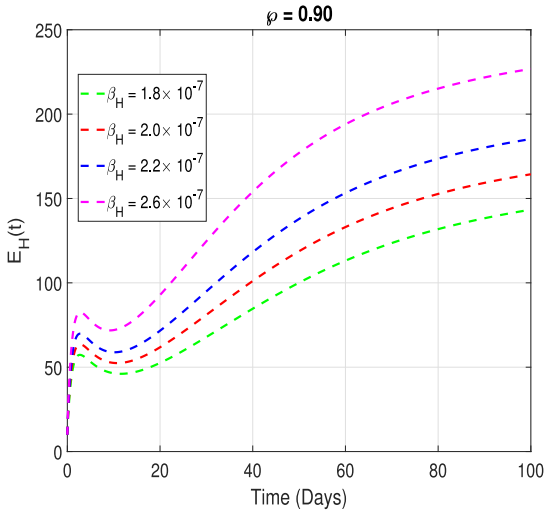

(a) The transmission pattern of $E_H(t)$ for several β_H points.

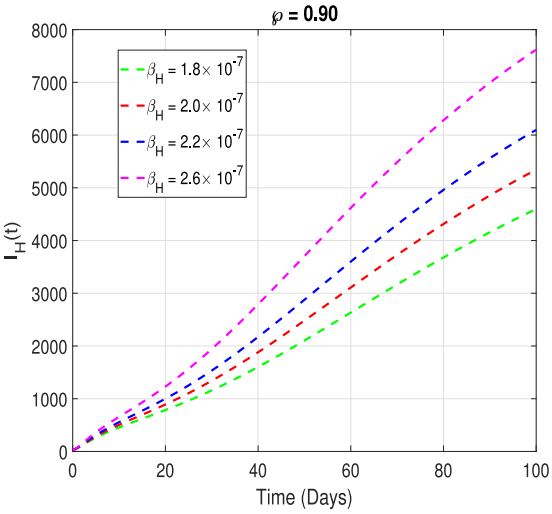

(b) The transmission pattern of $I_H(t)$ for several β_H points.

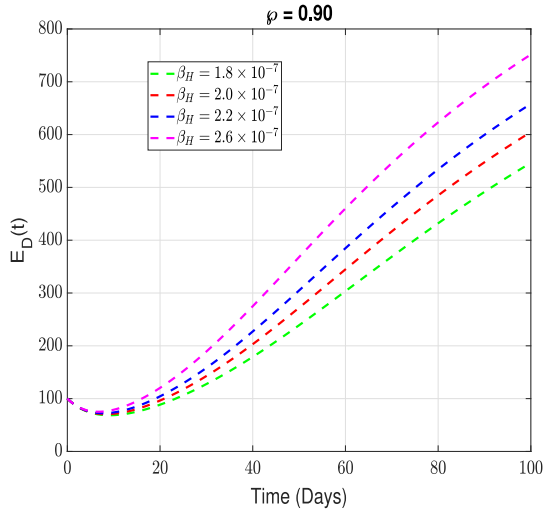

(c) The transmission pattern of $E_D(t)$ for several β_H points.

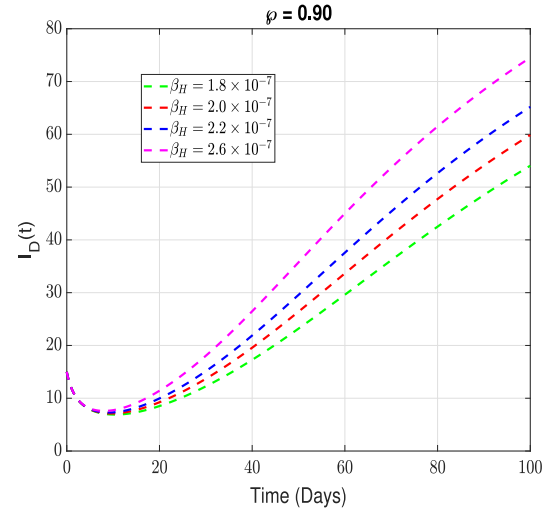

(d) The transmission pattern of $I_D(t)$ for several β_H points.

Fig. 6. The transmission patterns for $E_H(t), I_H(t), E_D(t), I_D(t)$ for several β_H values.

Table 4
Sensitivity analysis of the Ebola reproduction number with $\wp = 0.90$.

Parameters	Index	Parameters	Index
m_1	+0.5000	β_D	+0.5000
m_2	+0.5000	μ_D	−0.5026
σ_D	+0.0023	μ_H	−0.5000
σ_H	$+4.6465\times 10^{-4}$	γ_D	−0.4997
β_H	+0.5000	γ_H	−0.2040
δ_H	−0.9955		

we use the normalised forward sensitivity index of the Ebola reproduction number, $\mathcal{R}_0$. This is defined as:

$$X_{\mathcal{B}}^{\mathcal{R}_0} = \frac{\partial \mathcal{R}_0}{\partial \mathcal{B}} \times \frac{\mathcal{B}}{\mathcal{R}_0}, \tag{52}$$

where $\mathcal{B}$ is the individual parameters in the Ebola reproduction number. The respective forward sensitivity indexes using Eq. (52) and the parameter values in Table 3 are in Table 4.

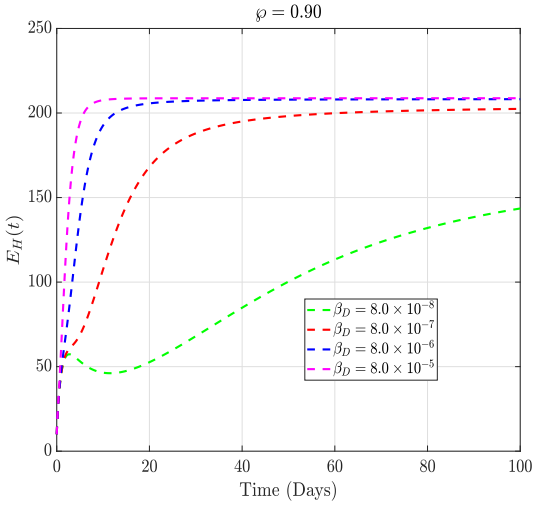

(a) The transmission pattern of $E_H(t)$ for several β_D points.

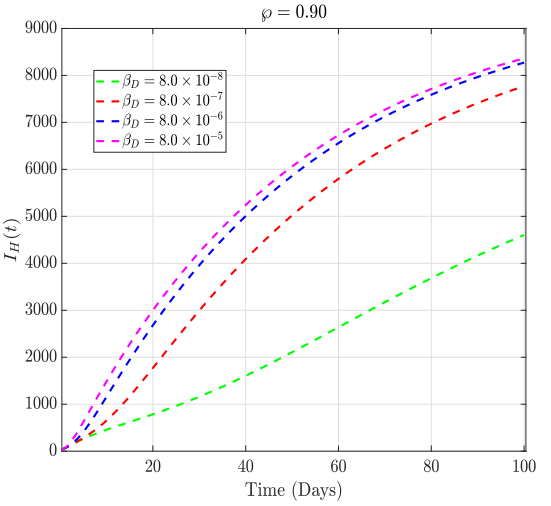

(b) The transmission pattern of $I_H(t)$ for several β_D points.

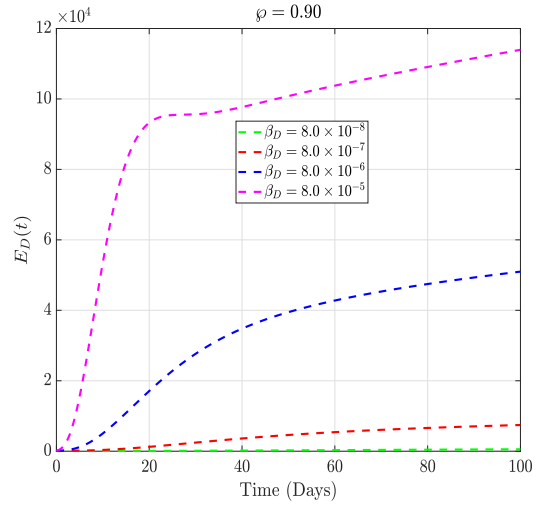

(c) The transmission pattern of $E_D(t)$ for several β_D points.

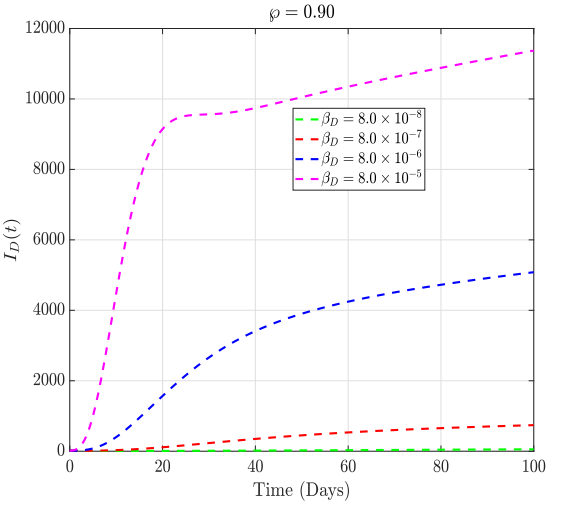

(d) The transmission pattern of $I_D(t)$ for several β_D points.

Fig. 7. The transmission patterns for $E_H(t), I_H(t), E_D(t), I_D(t)$ for several β_D values.

From Table 4, the parameters whose sensitivity indexes are negative decrease the value of $\mathcal{R}_0$ as their values increase, while those with positive signs increase the value of $\mathcal{R}_0$ as their values increase. The parameters with the most positive sensitive indexes in the obtained Ebola reproduction number are m_1, m_2, β_H, and β_D. For example, increasing(decreasing) the value of β_D, by 10% increases or decreases the value of $\mathcal{R}_0$ by 5%. In the same way, increasing or decreasing the value of γ_H by 10% increases or decreases the value of $\mathcal{R}_0$ by 2.040%. Also, increasing (or decreasing) the value of β_H and γ_D by 10% increases (or decreases) the value of $\mathcal{R}_0$ by 5% and 4.997% respectively.

Fig. 2 shows the sensitiveness corresponding changes in the $\mathcal{R}_0$, as some parameters ($\beta_H, \beta_D, \gamma_H, \gamma_D$ and σ_H) are varied together. From Fig. 2(a) it is noticed that, the value of $\mathcal{R}_0$ increases if β_H and σ_H increases. This indicates that, as the transmission rate in humans and Ebola incubation rate increases, respectively, the number of secondary infections increases in the community. Therefore, it informs that one can control the disease when the transmission rate in humans reduces, and the number of exposed individuals reduces. In Fig. 2(b), it is noticed that a significant increase in the Ebola transmission rate in dogs increases the number of secondary infections irrespective of the recovery rate in dogs. This indicates that the best way to control Ebola in the community is to reduce the transmission rate in dogs to reduce the corresponding transition to the human population. In Fig. 2(c), it is noticed that an increase in the recovery rate of humans reduces the number of secondary infections. In Fig. 2(d), it is noticed that an increase in both recovery rates in the human and dog population reduces the number of secondary infections. However, the recovery rate in

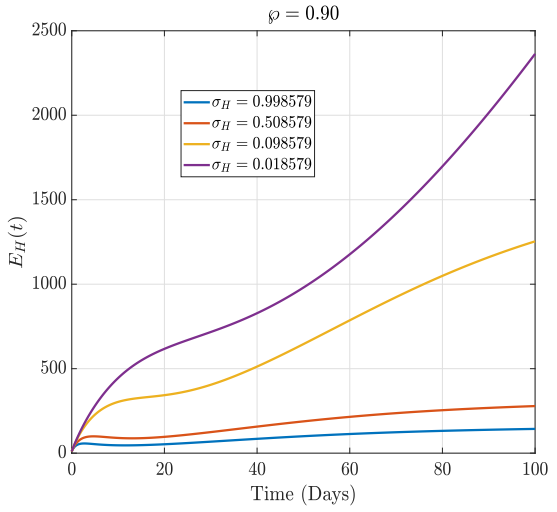

(a) The transmission pattern of $E_H(t)$ for several σ_H points.

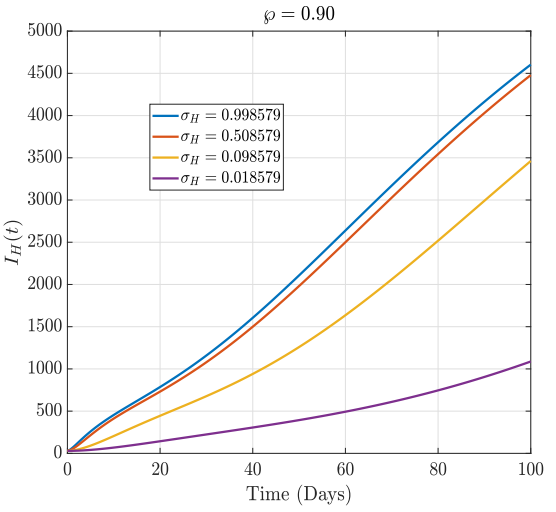

(b) The transmission pattern of $I_H(t)$ for several σ_H points.

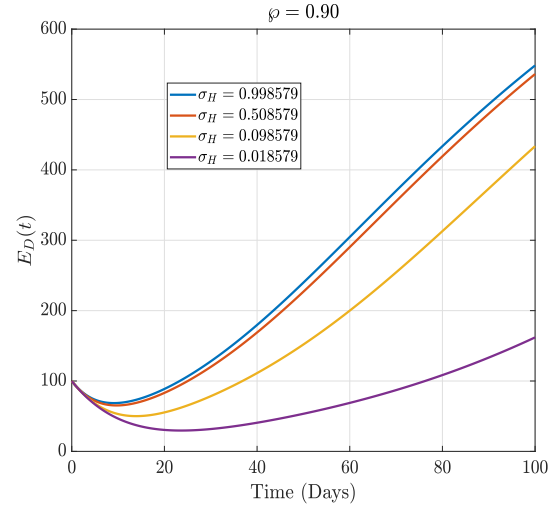

(c) The transmission pattern of $E_D(t)$ for several σ_H points.

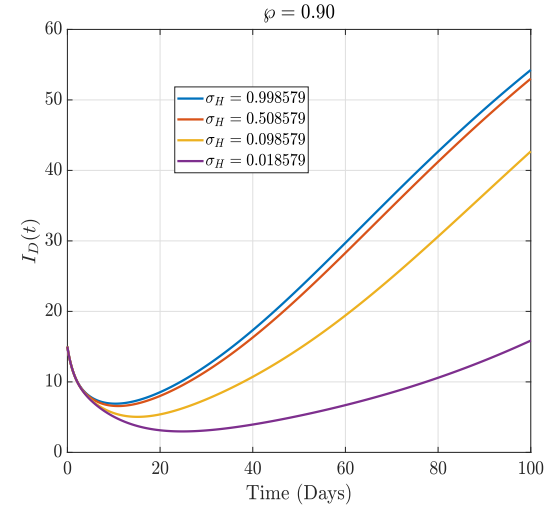

(d) The transmission pattern of $I_H(t)$ for several σ_H points.

Fig. 8. The transmission pattern of $I_H(t), E_H(t), I_D(t), E_D(t)$ for several σ_H points.

the human population has shown to be more dominant. Hence, a continuous improvement in the recovery of infected humans from Ebola will help reduce $\mathcal{R}_0$ to less than unity.

In Fig. 3 it is noticed that, there exist forward bifurcation. This means that the Ebola can be control when $\mathcal{R}_0 < 1$ and the Ebola will spread when $\mathcal{R}_0 > 1$. In Figs. 3(a) and 3(b), we used the transmission rate in dogs and the incubation rate in humans as our bifurcation parameters, respectively. Figs. 3(a) and 3(b) show that one can control Ebola whenever these parameters are controlled. In Figs. 4 and 5, we showed the impact of memory on the dynamics of Ebola. This pattern captures the events that happen before the integer order. It is noticed that the number of secondary infections reduces as memory (fractional order) changes, which informs that Ebola systematically reduces. Thus, the Caputo–Fabrizio fractional derivative employed here has characterised non-local and memory-dependent phenomena in the proposed Ebola human-dog model. Unlike classical derivatives, these represent events characterised by intricate dynamics, memory effects, and non-local behaviours. In Fig. 4(a), we observe that as the fractional order decreases over time, the number of susceptible humans increases. A decrease in the number of exposed humans, symptomatic humans, and recovery humans, see Figs. 4(b), 4(c), and 4(d), respectively. However, we noticed in Fig. 4(b) that, after day 8, a crossover effect exists in the exposed human compartment for about 12 days before reverting to the original pattern of decreasing the number of exposed humans as memory is changed. This may result from other factors in the exposed human compartment that memory cannot capture. In Fig. 5(a), we observe that as the fractional order decreases over time, the number of susceptible dogs decreases, and a decrease in the number of exposed dogs, symptomatic dogs, and recovery dogs, see Figs. 5(b), 5(c), and 5(d), respectively. However, we noticed in Figs. 5(b) and 5(c) that there exists a sharp crossover effect in the exposed dog compartment

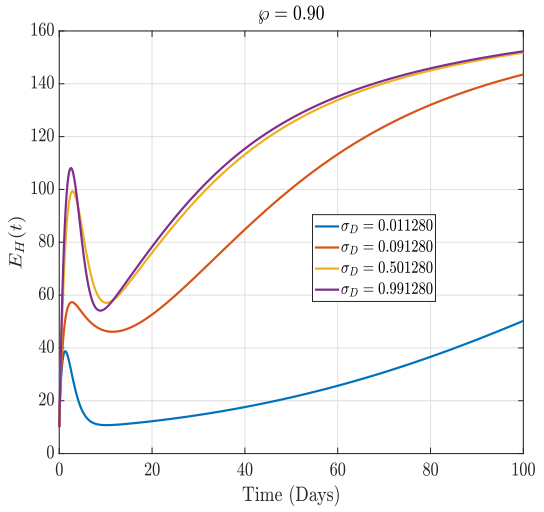

(a) The transmission pattern of $E_H(t)$ for several σ_D points.

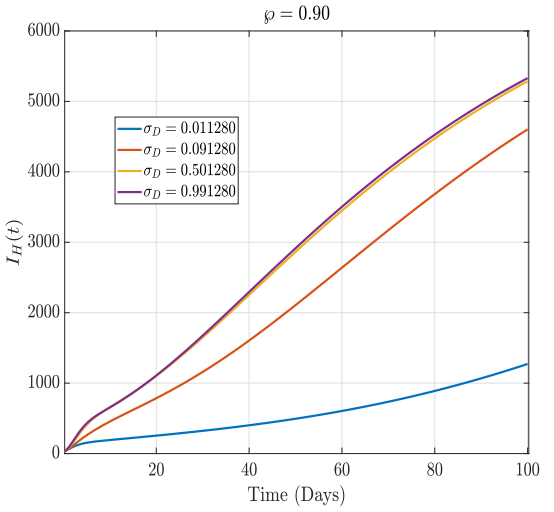

(b) The transmission pattern of $I_H(t)$ for several σ_D points.

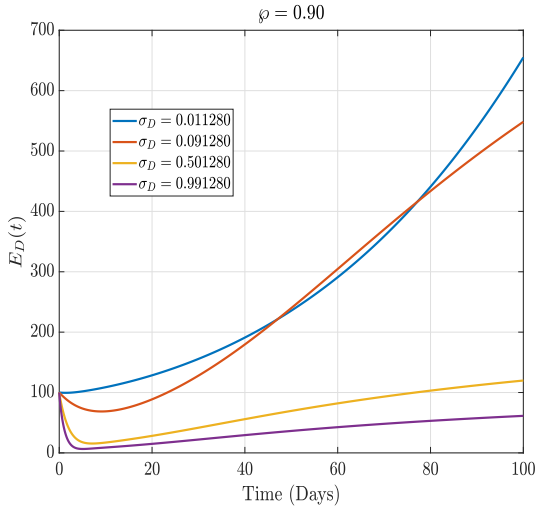

(c) The transmission pattern of $E_D(t)$ for several σ_D points.

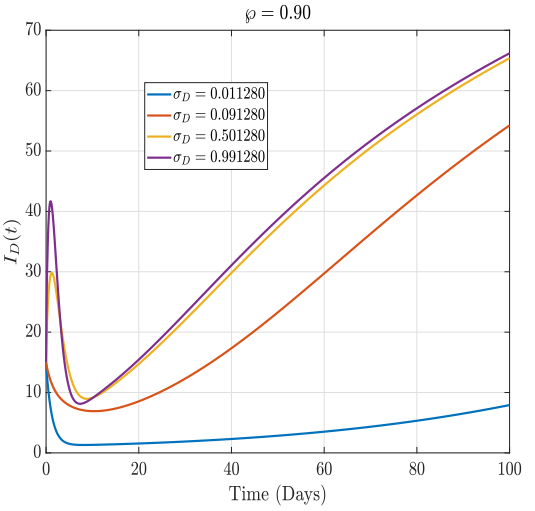

(d) The transmission pattern of $I_H(t)$ for several σ_D points.

Fig. 9. The transmission pattern of $I_H(t), E_H(t), I_D(t), E_D(t)$ for several σ_D points.

and symptomatic dog compartment between day 10 and day 20 before reverting to the original pattern of decreasing in the number of exposed dogs and symptomatic dogs as memory is changed. This may result from other factors in the exposed dog and symptomatic compartments, which memory cannot capture. In Figs. 6 and 7, we studied the events characterised by intricate dynamics, memory effects, and non-local behaviours when the fractional order is kept at $\wp = 0.90$. In Figs. 6(a), 6(b), 6(c), and 6(d), we noticed that, as one varies the transmission rate in humans, the trajectory behaviours of the number of exposed humans, symptomatic humans, exposed dogs and symptomatic dogs increases without crisscrossing. This indicates that each transmission rate needs effective measures to control the spread of Ebola in humans. In Figs. 7(a), 7(b), 7(c), and 7(d), we noticed that, as one varies the transmission rate in dogs, the trajectory behaviours of the number of exposed humans, symptomatic humans, exposed dogs and symptomatic dogs increases without crisscrossing. This indicates that, at each transmission rate, one needs effective measures to control the spread of Ebola in dogs. However, we noticed in Fig. 7(a) that, the transmission rate $\beta_D = 8.0\times10^{-6}$ and $\beta_D = 8.0\times10^{-5}$, attains same equilibrium after day 37. Implying that similar control measures could be used to reduce the transmission effects of $\beta_D = 8.0\times10^{-6}$ and $\beta_D = 8.0\times10^{-5}$ in the community. In Figs. 8 and 9, we studied the events characterised by the intricate dynamics, memory effects, and non-local behaviours of the time from when humans and dogs get infected to having symptoms when the fractional order is kept at $\wp = 0.90$. In Figs. 8(a), 8(b), 8(c), and 8(d), we noticed that, as one reduces the incubation rate in humans, the trajectory behaviours of the number of exposed humans increases, and that of symptomatic humans, exposed dogs and symptomatic dogs reduces without crisscrossing. This indicates that, at each incubation rate, one needs effective measures to control the spread of Ebola in humans. In Figs. 9(a), 9(b), 9(c), and 9(d), we noticed that, as one increases the incubation rate in dogs, the

trajectory behaviours of the number of exposed humans, symptomatic humans, symptomatic dogs increase without crisscrossing. However, that of exposed dogs reduces. This indicates that, at each incubation rate, one needs effective measures to control the spread of Ebola in dogs. However, we noticed in Fig. 9(c) that, the incubation rate $\sigma_D = 0.011280$ and $\sigma_D = 0.091280$, crisscross after day 42 and before day 80. This implies that other factors may affect the exposed dog compartment, which memory cannot capture. Hence, the numerical simulation of the Caputo–Fabrizio fractional Ebola human-dog model suggests that the transmission of diseases could have non-local characteristics. The spread of Ebola human-dog transmission within a population can be affected by variables beyond close physical proximity, such as travel patterns or linkages between distant people.

Conclusion

The present study aimed to examine the transmission dynamics of Ebola through the Caputo–Fabrizio fractional operator. The two-step Lagrange interpolation method was employed to simulate the model for various fractional order values. The existence of a solution for the Ebola model was established using the fixed-point theory. Furthermore, we engaged in a discussion regarding the distinctiveness of the answers to the model. Once again, we have demonstrated the Picard $\Psi-$ stability of the Ebola model under investigation using the Sumudu transform criterion. The impact of natural phenomena in the physical environment on the disease dynamics was carefully observed. Our analysis examined various fractional values, specifically $\wp = 0.90, 0.80, 0.70, 0.60, 0.50,$ and 0.40, compared to the integer order $\wp = 1$. We also observed a decline in infections as the fractional order decreased. Again, we considered varying the values of the sensitive parameters to observe how significantly they influence the model. We realised that as the contact rates among humans increased during the disease outbreak, many individuals became infected. This indicates that we need to employ quarantine and isolation to decrease the interactions among the exposed and infected individuals. Also, we observed that as many individuals develop antibodies that could resist the disease, the number of infections drastically reduces. Therefore, we implore health workers to educate individuals in the population to keep their immune systems strong to resist infections. This research suggests that scientists consider the development of efficient antibody-based remedies to control the spread of Ebola among people. In the future, we hope to study the dynamics of Ebola using fractal-fractional dynamics in non-constant populations.

Research funding

No funding

CRediT authorship contribution statement

Isaac K. Adu: Conceptualization, Investigation, Formal analysis, Writing – review & editing. **Fredrick A. Wireko:** Conceptualization, Investigation, Formal analysis, Writing – review & editing. **Mojeeb Al-R. El-N. Osman:** Formal analysis, Writing – review & editing. **Joshua Kiddy K. Asamoah:** Supervision, Investigation, Formal analysis, Model fitting, Writing – review & editing.

Declaration of competing interest

The authors declare that they have no known competing financial interests or personal relationships that could have appeared to influence the work reported in this paper.

Data availability

The data used for the research is described in the article.

Acknowledgements

The authors would like to say thanks to their respective universities for the production of this manuscript.

References

[1] H. Weingartl, C. Nfon, G. Kobinger, Review of Ebola virus infections in domestic animals, in: Vaccines and Diagnostics for Transboundary Animal Diseases, Vol. 135, Karger Publishers, 2013, pp. 211–218.
[2] L. Allela, O. Bourry, R. Pouillot, A. Délicat, P. Yaba, B. Kumulungui, P. Rouquet, J.-P. Gonzalez, E.M. Leroy, Ebola virus antibody prevalence in dogs and human risk, Emerg. Infect. Dis. 11 (3) (2005) 385.
[3] S. Gumusova, M. Sunbul, H. Leblebicioglu, Ebola virus disease and the veterinary perspective, Ann. Clin. Microbiol. Antimicrob. 14 (1) (2015) 1–5.
[4] E.M. Leroy, B. Kumulungui, X. Pourrut, P. Rouquet, A. Hassanin, P. Yaba, A. Délicat, J.T. Paweska, J.-P. Gonzalez, R. Swanepoel, Fruit bats as reservoirs of Ebola virus, Nature 438 (7068) (2005) 575–576.
[5] M. Penkowa, Dogs & Human Health: The New Science of Dog Therapy & Therapy Dogs, Balboa Press, 2015.
[6] A. Rachah, D.F. Torres, Mathematical modelling, simulation, and optimal control of the 2014 Ebola outbreak in West Africa, Discrete Dyn. Nat. Soc. 2015 (2015).
[7] I. Area, H. Batarfi, J. Losada, J.J. Nieto, W. Shammakh, Á. Torres, On a fractional order Ebola epidemic model, Adv. Difference Equ. 2015 (1) (2015) 1–12.
[8] X.-S. Wang, L. Zhong, Ebola outbreak in West Africa: real-time estimation and multiple-wave prediction, 2015, arXiv preprint arXiv:1503.06908.

[9] X. Pourrut, M. Souris, J.S. Towner, P.E. Rollin, S.T. Nichol, J.-P. Gonzalez, E. Leroy, Large serological survey showing cocirculation of Ebola and Marburg viruses in Gabonese bat populations, and a high seroprevalence of both viruses in Rousettus aegyptiacus, BMC Infect. Dis. 9 (1) (2009) 1–10.
[10] C.L. Althaus, Estimating the reproduction number of Ebola virus (EBOV) during the 2014 outbreak in West Africa, PLoS Curr. 6 (2014).
[11] G. Chowell, N.W. Hengartner, C. Castillo-Chavez, P.W. Fenimore, J.M. Hyman, The basic reproductive number of Ebola and the effects of public health measures: the cases of Congo and Uganda, J. Theoret. Biol. 229 (1) (2004) 119–126.
[12] J.-M. Zhu, L. Wang, J.-B. Liu, Eradication of Ebola based on dynamic programming, Comput. Math. Methods Med. 2016 (2016).
[13] M. Farman, A. Akgül, T. Abdeljawad, P.A. Naik, N. Bukhari, A. Ahmad, Modeling and analysis of fractional order Ebola virus model with Mittag-Leffler kernel, Alex. Eng. J. 61 (3) (2022) 2062–2073.
[14] M. Almuqrin, P. Goswami, S. Sharma, I. Khan, R. Dubey, A. Khan, Fractional model of Ebola virus in population of bats in frame of Atangana-Baleanu fractional derivative, Results Phys. 26 (2021) 104295.
[15] W. Pan, T. Li, S. Ali, A fractional order epidemic model for the simulation of outbreaks of Ebola, Adv. Difference Equ. 2021 (1) (2021) 1–21.
[16] H. Singh, Analysis for fractional dynamics of Ebola virus model, Chaos Solitons Fractals 138 (2020) 109992.
[17] F.A. Wireko, I.K. Adu, C. Sebil, J.K.K. Asamoah, A fractal–fractional order model for exploring the dynamics of Monkeypox disease, Decis. Anal. J. 8 (2023) 100300.
[18] L. Zhang, E. Addai, J. Ackora-Prah, Y.D. Arthur, J.K.K. Asamoah, Fractional-order Ebola-Malaria coinfection model with a focus on detection and treatment rate, Comput. Math. Methods Med. 2022 (2022).
[19] I.K. Adu, F.A. Wireko, C. Sebil, J.K.K. Asamoah, A fractal–fractional model of Ebola with reinfection, Results Phys. 52 (2023) 106893.
[20] A. Raza, M. Farman, A. Akgül, M.S. Iqbal, A. Ahmad, et al., Simulation and numerical solution of fractional order Ebola virus model with novel technique, AIMS Bioeng. 7 (4) (2020) 194–207.
[21] M.A. Dokuyucu, H. Dutta, A fractional order model for Ebola Virus with the new Caputo fractional derivative without singular kernel, Chaos Solitons Fractals 134 (2020) 109717.
[22] A.A. Thirthar, R.K. Naji, F. Bozkurt, A. Yousef, Modeling and analysis of an SI1I2R epidemic model with nonlinear incidence and general recovery functions of I1, Chaos Solitons Fractals 145 (2021) 110746.
[23] J.K.K. Asamoah, Fractal–fractional model and numerical scheme based on Newton polynomial for Q fever disease under Atangana–Baleanu derivative, Results Phys. 34 (2022) 105189.
[24] A.A. Thirthar, S.J. Majeed, K. Shah, T. Abdeljawad, The dynamics of an aquatic ecological model with aggregation, Fear and Harvesting Effects, AIMS Math. 7 (10) (2022) 18532–18552.
[25] J.K.K. Asamoah, G.-Q. Sun, Fractional Caputo and sensitivity heat map for a gonorrhea transmission model in a sex structured population, Chaos Solitons Fractals 175 (2023) 114026.
[26] A. Yousef, A.A. Thirthar, A.L. Alaoui, P. Panja, T. Abdeljawad, The hunting cooperation of a predator under two prey's competition and fear-effect in the prey-predator fractional-order model, AIMS Math. 7 (4) (2022) 5463–5479.
[27] A.A. Thirthar, H. Abboubakar, A. Khan, T. Abdeljawad, Mathematical modeling of the COVID-19 epidemic with fear impact, AIMS Math. 8 (3) (2023) 6447–6465.
[28] J. Ackora-Prah, B. Seidu, E. Okyere, J.K. Asamoah, Fractal-fractional Caputo maize streak virus disease model, Fractal Fract. 7 (2) (2023) 189.
[29] J.K. Asamoah, E. Addai, Y.D. Arthur, E. Okyere, A fractional mathematical model for listeriosis infection using two kernels, Decis. Anal. J. 6 (2023) 100191.
[30] E. Addai, L. Zhang, A.K. Preko, J.K.K. Asamoah, Fractional order epidemiological model of SARS-CoV-2 dynamism involving Alzheimer's disease, Healthc. Anal. 2 (2022) 100114.
[31] M.A. Khan, K. Shah, Y. Khan, S. Islam, Mathematical modeling approach to the transmission dynamics of pine wilt disease with saturated incidence rate, Int. J. Biomath. 11 (03) (2018) 1850035.
[32] M. Caputo, M. Fabrizio, A new definition of fractional derivative without singular kernel, Prog. Fract. Differ. Appl. 1 (2) (2015) 73–85.
[33] J. Losada, J.J. Nieto, Properties of a new fractional derivative without singular kernel, Progr. Fract. Differ. Appl 1 (2) (2015) 87–92.
[34] F.B.M. Belgacem, A.A. Karaballi, S.L. Kalla, Analytical investigations of the Sumudu transform and applications to integral production equations, Math. Probl. Eng. 2003 (3) (2003) 103–118.
[35] D. Bodkhe, S. Panchal, On Sumudu transform of fractional derivatives and its applications to fractional differential equations, Asian J. Math. Comput. Res. 11 (1) (2016) 69–77.
[36] K. Shah, M. Junaid, N. Ali, Extraction of Laplace, Sumudu, Fourier and Mellin transform from the natural transform, J. Appl. Environ. Biol. Sci. 5 (9) (2015) 108–115.
[37] G. Watugala, Sumudu transform: a new integral transform to solve differential equations and control engineering problems, Integr. Educ. 24 (1) (1993) 35–43.
[38] E. Leroy, J. Gonzalez, X. Pourrut, Ebolavirus and other filoviruses, in: Wildlife and Emerging Zoonotic Diseases: The biology, circumstances and consequences of cross-species transmission, Springer, 2007, pp. 363–387.
[39] Z. EL Rhoubari, H. Besbassi, K. Hattaf, N. Yousfi, Mathematical modeling of Ebola virus disease in bat population, Discrete Dyn. Nat. Soc. 2018 (2018) 1–7.
[40] L. Esteva, M. Matias, A model for vector transmitted diseases with saturation incidence, J. Biol. Systems 9 (04) (2001) 235–245.
[41] B. Seidu, J.K.K. Asamoah, E.N. Wiah, J. Ackora-Prah, A comprehensive cost-effectiveness analysis of control of maize streak virus disease with Holling's Type II predation form and standard incidence, Results Phys. 40 (2022) 105862.
[42] V.E. Tarasov, Caputo–Fabrizio operator in terms of integer derivatives: memory or distributed lag? Comput. Appl. Math. 38 (2019) 1–15.
[43] M. Farman, R. Sarwar, A. Akgul, Modeling and analysis of sustainable approach for dynamics of infections in plant virus with fractal fractional operator, Chaos Solitons Fractals 170 (2023) 113373.
[44] A. Atangana, Mathematical model of survival of fractional calculus, critics and their impact: How singular is our world? Adv. Difference Equ. 2021 (1) (2021) 1–59.
[45] A. Atangana, S. İğret Araz, Mathematical model of COVID-19 spread in Turkey and South Africa: theory, methods, and applications, Adv. Difference Equ. 2020 (1) (2020) 1–89.
[46] A. Atangana, Modelling the spread of COVID-19 with new fractal-fractional operators: can the lockdown save mankind before vaccination? Chaos Solitons Fractals 136 (2020) 109860.
[47] R. Shi, H. Zhao, S. Tang, Global dynamic analysis of a vector-borne plant disease model, Adv. Difference Equ. 2014 (1) (2014) 1–16.
[48] A. Mwasa, J.M. Tchuenche, Mathematical analysis of a cholera model with public health interventions, Biosystems 105 (3) (2011) 190–200.
[49] O. Diekmann, J.A.P. Heesterbeek, J.A. Metz, On the definition and the computation of the basic reproduction ratio R 0 in models for infectious diseases in heterogeneous populations, J. Math. Biol. 28 (1990) 365–382.
[50] P. Van den Driessche, J. Watmough, Reproduction numbers and sub-threshold endemic equilibria for compartmental models of disease transmission, Math. Biosci. 180 (1–2) (2002) 29–48.
[51] J.K.K. Asamoah, F. Nyabadza, B. Seidu, M. Chand, H. Dutta, Mathematical modelling of bacterial meningitis transmission dynamics with control measures, Comput. Math. Methods Med. 2018 (2018).

[52] J.K.K. Asamoah, F.T. Oduro, E. Bonyah, B. Seidu, et al., Modelling of rabies transmission dynamics using optimal control analysis, J. Appl. Math. 2017 (2017).
[53] J. Carr, Applications of Centre Manifold Theory, Tech. Rep., Brown Univ Providence Ri Lefschetz Center For Dynamical Systems, 1979.
[54] A.P. Lemos-Paião, C.J. Silva, D.F. Torres, An epidemic model for cholera with optimal control treatment, J. Comput. Appl. Math. 318 (2017) 168–180.
[55] C. Castillo-Chavez, B. Song, Dynamical models of tuberculosis and their applications, Math. Biosci. Eng. 1 (2) (2004) 361–404.
[56] J. Luo, W. Wang, H. Chen, R. Fu, Bifurcations of a mathematical model for HIV dynamics, J. Math. Anal. Appl. 434 (1) (2016) 837–857.
[57] B. Buonomo, D. Lacitignola, On the backward bifurcation of a vaccination model with nonlinear incidence, Nonlinear Anal. Model. Control 16 (1) (2011) 30–46.
[58] J.K.K. Asamoah, M.A. Owusu, Z. Jin, F. Oduro, A. Abidemi, E.O. Gyasi, Global stability and cost-effectiveness analysis of COVID-19 considering the impact of the environment: using data from Ghana, Chaos Solitons Fractals 140 (2020) 110103.
[59] J.K.K. Asamoah, Z. Jin, G.-Q. Sun, B. Seidu, E. Yankson, A. Abidemi, F. Oduro, S.E. Moore, E. Okyere, Sensitivity assessment and optimal economic evaluation of a new COVID-19 compartmental epidemic model with control interventions, Chaos Solitons Fractals 146 (2021) 110885.
[60] S. Uçar, Analysis of hepatitis B disease with fractal–fractional Caputo derivative using real data from Turkey, J. Comput. Appl. Math. 419 (2023) 114692.
[61] G. Chowell, J.M. Hyman, L.M. Bettencourt, C. Castillo-Chavez, Mathematical and Statistical Estimation Approaches in Epidemiology, Springer, 2009.
[62] M. Martcheva, An Introduction to Mathematical Epidemiology, Vol. 61, Springer, 2015.
[63] J.K.K. Asamoah, et al., A fractional mathematical model of heartwater transmission dynamics considering nymph and adult amblyomma ticks, Chaos Solitons Fractals 174 (2023) 113905.
[64] F. Branda, A. Maruotti, 2022 Uganda Ebola outbreak: Early descriptions and open data, J. Med. Virol. 95 (1) (2023) e28344, URL https://github.com/fbranda/ebola.
[65] F. Branda, A. Mahal, A. Maruotti, M. Pierini, S. Mazzoli, The challenges of open data for future epidemic preparedness: The experience of the 2022 Ebolavirus outbreak in Uganda, Front. Pharmacol. 14 (2023) 1101894, URL https://raw.githubusercontent.com/fbranda/ebola/main/Surveillance_data_Ebola_outbreak.csv.
[66] worldometer, Worldometers.info/world-population/uganda-population, 2023, https://www.worldometers.info/world-population/uganda-population/, (Accessed 20 December 2023).
[67] WHO, Ebola virus disease, 2023, https://www.who.int/news-room/fact-sheets/detail/ebola-virus-disease, (Accessed 20 December 2023).
[68] macrotrends, Uganda life expectancy 1950–2023, 2023, https://www.macrotrends.net/countries/UGA/uganda/life-expectancy, (Accessed 20 December 2023).
[69] R.M. Wallace, J. Mehal, Y. Nakazawa, S. Recuenco, B. Bakamutumaho, M. Osinubi, V. Tugumizemu, J.D. Blanton, A. Gilbert, J. Wamala, The impact of poverty on dog ownership and access to canine rabies vaccination: results from a knowledge, attitudes and practices survey, Uganda 2013, Infect. Dis. Poverty 6 (2017) 1–22.
[70] K. Genetics, Village Dog Uganda-dog breed test, 2023, https://www.kokogenetics.com/en/results/dog-dna-test-breed/village-dog-uganda, (Accessed 20 December 2023).
[71] T. Berge, A. Ouemba Tassé, H. Tenkam, J. Lubuma, Mathematical modeling of contact tracing as a control strategy of Ebola virus disease, Int. J. Biomath. 11 (07) (2018) 1850093.
[72] J.K.K. Asamoah, F. Nyabadza, Z. Jin, E. Bonyah, M.A. Khan, M.Y. Li, T. Hayat, Backward bifurcation and sensitivity analysis for bacterial meningitis transmission dynamics with a nonlinear recovery rate, Chaos Solitons Fractals 140 (2020) 110237.